Finite-strain Landau theory applied to the high-pressure phase transition of lead titanate

A. Tröster,[1,*] S. Ehsan,[1] K. Belbase,[1] P. Blaha,[1] J. Kreisel,[2,3] and W. Schranz[4]

[1]*Vienna University of Technology, Institute of Material Chemistry, Getreidemarkt 9, A-1060 Wien, Austria*

[2]*Department of Materials Research and Technology, Luxembourg Institute of Science and Technology, 41 Rue du Brill, L-4422 Belvaux, Luxembourg*

[3]*Physics and Materials Science Research Unit, University of Luxembourg, 41 Rue du Brill, L-4422 Belvaux, Luxembourg*

[4]*University of Vienna, Boltzmanngasse 5, A-1090 Vienna, Austria*

(Received 29 November 2016; revised manuscript received 6 February 2017; published 27 February 2017)

Standard Landau theory coupled to infinitesimal strain allows a concise description of the temperature-driven ferroelectric tetragonal-to-cubic phase transition in $PbTiO_3$ at ambient pressure. Unfortunately, it fails to cover its high-pressure counterpart at ambient temperature. For example, the experimental transition pressure is vastly underestimated, and neither the change from first to second order with increasing pressure nor the unusual pressure dependence of the tetragonal unit cell parameters observed in experiment are reproduced. Here we demonstrate that a combination of density functional theory and a recently constructed finite-strain extension of Landau theory provides a natural mechanism for resolving these discrepancies between theory and experiment. Our approach also allows us to determine the full tetragonal-cubic phase boundary in the (P,T) plane including an estimate of the tricritical point. We show that a careful analysis of the thermal elastic baseline is an essential ingredient to the success of this theory.

DOI: 10.1103/PhysRevB.95.064111

I. INTRODUCTION

Understanding the combined effects of temperature and pressure in inducing structural phase transitions is of vital interest to a large range of scientific disciplines. In particular, the study of crystals of perovskite type with structural formula ABX_3 (A=Ba, Ca, Mg, Pb, Sr, Ln, Y, ..., B=Ti, Zr, Si, La, Mn, etc., X=O, F) attracts a major interest, in both materials research and earth science. As to the latter, a prominent example is the perovskite-postperovskite transition in $(Mg,Fe)SiO_3$. It was the discovery of this transition [1], which occurs only at extreme pressures up to 125 GPa and temperatures of some 2500 K, that finally elucidated the unusual seismic properties of the earth's core-mantle D″ boundary layer. In addition to external hydrostatic pressure [2], electronic, magnetic, and optical properties of materials may also be strongly affected by chemical pressure [3] or uniaxial stress [4]. High pressure also plays an important role in the synthesis of bulk multiferroic materials and provides insight into the complex interplay between magnetic and electronic properties and structural instabilities [5].

The paradigm formed by traditional Landau theory (LT) [6,7] and the closely related lattice-dynamical theory of "soft modes" [8] is a cornerstone of our understanding of structural phase transitions. In transitions driven by changing the temperature at ambient pressure, strain effects are usually small enough to warrant a harmonic treatment of the elastic contributions to the Landau potential (LP), and this approach also works for transitions driven by moderate external stress. However, the last two decades have seen a rapid improvement of the experimental capabilities for studying materials at extreme pressures [9]. It has become routine to control stresses that frequently represent sizable fractions of the elastic constants of the materials investigated. Under such conditions, a description of pressure-induced transitions based on linear elasticity is bound to fail. A pressing need arises for an adequate extension of traditional LT to include nonlinear elastic effects at high stress and strain.

In Ref. [10] such a high-pressure extension of an existing ambient-pressure LP has been constructed. The most important input required by this finite-strain Landau theory (FSLT) is a set of pressure-dependent elastic constants of the high-symmetry phase which are calculated from density functional theory (DFT). Introducing additional parameters to capture the remaining nonlinear pressure evolution of the order parameter–strain coupling coefficients then allows to give a concise numerical description of the room-temperature high-pressure phase transition $Pm\bar{3}m \leftrightarrow I4/mcm$ of the archetype perovskite strontium titanate $SrTiO_3$ (STO) whereas a traditional Landau approach based on truncating the elastic energy at harmonic order fails quantitatively.

The purpose of the present paper is threefold. First, it illustrates the capabilities of our theory for the example of lead titanate $PbTiO_3$ (PTO). As we shall demonstrate below, traditional LT fails in this case not only on the quantitative but even on the qualitative level.

Of course, it would be desirable to work out a true *ab initio* description [11,12] rather than relying on a theory that involves both input from DFT and a certain number of free parameters that need to be determined from fits to experimental data. However, electronic structure methods like DFT reside at zero temperature. Imposing an arbitrary external pressure poses no particular problem in DFT, but including effects of high temperatures is difficult. On the other hand, experimentalists have accumulated a wealth of data on the temperature dependence of structural phase transitions and encoded them in terms of published sets of numerical parameters for the corresponding LPs over the years (for ferroelectric perovskites see, e.g., Appendix A of Ref. [13]). Our second goal is to present FSLT as a general framework for extending this thermal information from ambient to high pressure.

*andreas.troester@tuwien.ac.at

Third, we shall see that separating spontaneous and background strain must be done carefully when extracting Landau parameters from experimental data.

The paper is organized as follows. Section II presents a critical survey of the main predictions obtained from conventional LT for PTO. Section III reviews basic FSLT. Finite-temperature effects are treated in Sec. IV. Section V is devoted to the application to PTO. Section VI closes the paper with a discussion of results. Some technical arguments with the potential of distracting the reader's attention from the paper's main objective are gathered in Appendices A–D.

II. SURVEY OF EXISTING RESULTS FOR THE FERROELECTRIC TRANSITION OF LEAD TITANATE

PTO is one of the most extensively studied ferroelectrics and is generally considered as a model material for understanding structural phase transitions. Moreover, PTO is an end member of high piezoelectric materials [14] like $PbZr_{1-x}(TiO_3)_x$ (PZT) or $(PbMg_{1/3}Nb_{2/3}O_3)_{1-x}(TiO_3)_x$ (PMN-PT), both of which exhibit a giant electromechanical (piezoelectric) response [15] near the so-called morphotropic phase boundary. They are thus of great technological importance. In view of the vast amount of literature on PTO, here, we only provide a short summary of results that are relevant for the present work.

Our focus is on the ferroelectric displacive transition from the tetragonal space group $P4mm$ to the prototypical cubic perovskite structure $Pm\bar{3}m$. At ambient pressure, this transition is of first order at a reported Curie temperature of $T_c \approx 492\,^{\circ}$C. Following its discovery in 1950 [16,17], the underlying soft-mode dynamics was studied by neutron scattering [18] and Raman spectroscopy [19,20]. Guided by previous work [21,22], Haun *et al.* [23] constructed a Landau-Devonshire theory [24] that accounts for all possible [25] transitions from the cubic parent phase to tetragonal, orthorhombic, or rhombohedral phases under application of external stress. In what follows, we shall use small Latin letters for 3d vector indices $i,j,\ldots = 1,2,3$ and Greek ones $\mu,\nu,\ldots = 1,\ldots,6$ for Voigt indices. Using this convention, the phenomenological Gibbs potential density of Haun *et al.* includes all symmetry-allowed polynomial invariants up to sixth order built from the three components P_i of the spontaneous polarization $\boldsymbol{P}$ that serves as the primary order parameter (OP), linear-quadratic couplings between the components σ_μ of the external stress and the primary OP components, as well as a "bare" harmonic elastic energy. We shall focus on a single domain description by setting $P_1 = P_2 = 0$, with P_3 playing the role of the primary OP. Then it suffices to work with the Gibbs potential density

$$G(P_3,\sigma_1,\sigma_2,\sigma_3) = G(P_3) + G_c(P_3,\sigma_1,\sigma_2,\sigma_3) + G_0(\sigma_1,\sigma_2,\sigma_3), \tag{1}$$

where

$$G(P_3) = \alpha_1 P_3^2 + \alpha_{11} P_3^4 + \alpha_{111} P_3^6, \tag{2a}$$

$$G_c(P_3,\sigma_1,\sigma_2,\sigma_3) = -P_3^2 \sum_\mu q_\mu \sigma_\mu, \tag{2b}$$

$$G_0(\sigma_1,\sigma_2,\sigma_3) = -\frac{1}{2}\sum_{\mu,\nu=1}^{3} S^0_{\mu\nu}\sigma_\mu\sigma_\nu. \tag{2c}$$

TABLE I. Landau parameter values used in our present calculations for dimensionless order parameter Q. The compliance components S^0_{11} and S^0_{12} are taken from Ref. [26] and agree with those listed in Table I of Gao *et al.* [27] or Table 5 on p. 368 of Ref. [13].

Parameter	Value
$\widehat{\alpha}_1$	7.644×10^{-4} GPa K^{-1} $\times (T_0 - T)$
T_0	751.95 K
$\widehat{\alpha}_{11}$	-7.252×10^{-2} GPa
$\widehat{\alpha}_{111}$	2.602×10^{-1} GPa
$\widehat{q}_{11}$	8.92×10^{-2}
$\widehat{q}_{12}$	-2.6×10^{-2}
S^0_{11}	8.0×10^{-12} Pa
S^0_{12}	-2.5×10^{-12} Pa

Here $S^0_{\mu\nu}$ are the bare elastic compliances of the cubic high-symmetry phase and $q_1 = q_2 = q_{12}$, $q_3 = q_{11}$ in the parametrization of Haun *et al.* In Ref. [23] numerical values for the parameters $\alpha_1,\alpha_{11},\alpha_{111},q_{11},q_{12}$ are given. Their behavior follows the traditional Landau prescription; i.e., α_1 depends linearly on temperature while all other coefficients are independent of T. The polarization P_3 has dimension C/m^2. In the present context, however, we prefer to work with a dimensionless OP instead, since the coupling coefficients then acquire the same units as the pressure. Rescaling $P_3 \equiv 1\text{C/m}^2 \cdot Q$, the coefficients $\alpha_1,\alpha_{11},\alpha_{111}$ and q_μ get replaced by rescaled versions $\hat{\alpha}_1,\hat{\alpha}_{11},\hat{\alpha}_{111}$ and $\hat{q}_\mu$. Table I lists those rescaled parameters that are needed in our present context.

Instead of stresses, FSLT requires a parametrization in terms of strains. Mathematically, this amounts to replacing the Gibbs by the Helmholtz potential by performing a partial Legendre transform

$$F(Q,\epsilon_1,\epsilon_2,\epsilon_3) = G(Q,\underline{\bar{\sigma}}(\underline{\epsilon})) + \sum_\mu \bar{\sigma}_\mu(\underline{\epsilon})\epsilon_\mu \tag{3}$$

of the LP of Haun *et al.* At fixed P, the required equilibrium strains are

$$\bar{\epsilon}_\mu = -\frac{\partial G}{\partial \sigma_\mu} = Q^2\widehat{q}_\mu + \sum_{\nu=1}^{3} S^0_{\mu\nu}\sigma_\nu. \tag{4}$$

Solving (4) for $\bar{\sigma}_\mu = \sum_\alpha C^0_{\mu\alpha}(\epsilon_\alpha - \widehat{q}_\alpha Q^2)$ where $C^0_{\mu\alpha}$ denote the cubic elastic constants, we find

$$F(Q,\epsilon_1,\epsilon_2,\epsilon_3) = G(Q) - Q^2\sum_{\alpha\beta} C^0_{\alpha\beta}\widehat{q}_\alpha\epsilon_\beta + \frac{Q^4}{2}\sum_{\mu,\alpha} q_\mu C^0_{\mu\alpha}\widehat{q}_\alpha + \frac{1}{2}\sum_{\alpha\beta} C^0_{\alpha\beta}\epsilon_\alpha\epsilon_\beta. \tag{5}$$

Using a more traditional parametrization, we obtain

$$F(Q,\epsilon_1,\epsilon_2,\epsilon_3) = \frac{A}{2}Q^2 + \frac{B}{4}Q^4 + \frac{C}{6}Q^6 + Q^2\sum_{\mu=} D_\mu\epsilon_\mu + \frac{1}{2}\sum_{\mu,\alpha}\epsilon_\mu C^0_{\mu\alpha}\epsilon_\nu, \tag{6}$$

where

$$A = 2\widehat{\alpha}_1, \tag{7}$$

$$B = 4\widehat{\alpha}_{11} + 2\sum_{\mu,\nu}\widehat{q}_\mu C^0_{\mu\nu}\widehat{q}_\alpha, \tag{8}$$

$$C = 6\widehat{\alpha}_{111}, \tag{9}$$

$$D_\mu = -\sum_\nu C^0_{\mu\nu}\widehat{q}_\nu. \tag{10}$$

Figures 4 and 5 of Ref. [23] suggest that for vanishing stress, the potential G (or equally F) is capable of offering a remarkable concise numerical description of both equilibrium OP as well as spontaneous strain components over a wide temperature range of nearly 500 K. In this parametrization the spontaneous strain components

$$\bar{\epsilon}_\mu(T) = \widehat{q}_\mu \bar{Q}^2(T) \tag{11}$$

appear to be exactly proportional over this temperature range with a T-independent proportionality factor $\widehat{q}_\mu$. In Refs. [13,26–28] the parameters published by Haun *et al.* in Ref. [23] have been taken over without any changes and can thus be regarded as well established in the literature. We shall reconsider the validity of this parametrization later on.

Unfortunately, the good agreement between data and theory for the temperature-driven transition at ambient pressure is spoiled for the pressure-driven case at ambient temperature. For hydrostatic stress $\sigma_{ij} = -P\delta_{ij}$ the above Landau Gibbs potential density becomes

$$G(Q,P) = -\frac{P^2}{2K_0} + [\alpha_1 + (2q_{12} + q_{11})P]Q^2 + \alpha_{11}Q^4 + \alpha_{111}Q^6, \tag{12}$$

where K_0 denotes the bulk modulus of the cubic parent phase. Note the linear P dependence of the harmonic contribution in contrast to the P independence of α_{11}. For $\alpha_{11} < 0$ this yields a first-order phase transition at

$$P_c^{\text{Haun}} = \frac{\widehat{\alpha}_1 + \frac{\widehat{\alpha}_{11}^2}{4\widehat{\alpha}_{111}}}{\widehat{q}_{11} + 2\widehat{q}_{12}} \tag{13}$$

with a corresponding OP discontinuity

$$\Delta Q_c = \sqrt{\frac{-\widehat{\alpha}_{11}}{2\widehat{\alpha}_{111}}} \tag{14}$$

at T_c and accompanying jumps

$$\Delta\epsilon_\mu = \Delta Q^2 \widehat{q}_\mu, \quad \mu = 1,2,3 \tag{15}$$

of the spontaneous strain components. Note that with the given parametrization these jumps are mere constants independent of both P and T. At room temperature T_R, the parameter values listed in Table I produce

$$P_c^{\text{Haun}}(T_R) = 2.92 \text{ GPa}, \tag{16a}$$

$$\Delta\epsilon_\mu^{\text{Haun}} = \begin{cases} -0.0036, & \mu = 1,2, \\ +0.0124, & \mu = 3. \end{cases} \tag{16b}$$

Our present work is motivated by the fact that these predictions are both qualitatively and quantitatively strikingly far from experiment. Instead, at room temperature in both the classic Raman study Ref. [29] and the high-pressure x-ray and Raman experiments conducted by Janolin *et al.* in Ref. [30] a second-order phase transition at a much larger critical pressure was detected.

In the single-crystal Raman experiments of Ref. [29], the merging of the tetragonal Raman-active $E(jTO)$ and $A_1(jTO)$ modes is observed at $P_c \approx 12$ GPa, beyond which they are reported to vanish abruptly. In addition, close to P_c the squared frequencies of the lowest modes $E(1TO)$ and $A_1(1TO)$ are found to vanish like $|P - P_c|$. Early x-ray diamond anvil cell experiments [31] on U-doped PTO confirmed the absence of any transition up to 6 GPa at room temperature and yielded a similar estimate for P_c. On pure PTO, both x-ray and Raman scattering measurements were finally carried out at room temperature in Ref. [30], covering a much larger pressure range from ambient pressure up to 63 GPa. Up to 12 GPa, the x-ray results are consistent with the $P4mm$ space group, while from 12 GPa to 20 GPa the unit cell parameters appear to be metrically cubic. The accompanying Raman data, which were obtained from powder, point more towards $P_c \approx 13$ GPa but also show some features that are not well understood. Nevertheless, the fact that some Raman modes continue to be observed above this pressure and are found to harden again is not necessarily incompatible with the assignment of the prototypical cubic perovskite structure $Pm\bar{3}m$ to this cubic phase. Similar observations are also made in the Raman spectra of $BaTiO_3$ and $KNbO_3$ (KNO) and are attributed to the existence of so-called nanopolar regions (cf. Ref. [32] and references therein). Summarizing, there is little doubt [33] that at room temperature lead titanate is of $Pm\bar{3}m$ symmetry within the pressure range of 12–20 GPa. In passing we note that above 20 GPa, further tetragonal phases are reported in Ref. [30], which hints at the rather complicated topology of the full phase diagram of PTO in the (P,T) plane [34]. Concise DFT calculations [35] reveal that at zero temperature a tetragonal ground state is followed by monoclinic and rhombohedral phases, but below some 200 K the existence of a cubic phase seems to be ruled out [34].

In quantitative terms, a discrepancy of some 300% between the experimentally observed critical pressure P_c and the prediction P_c^{Haun} deduced from the theory of Haun *et al.* should be sufficient to make advocates of the traditional Landau approach scratch their heads. To illustrate the even more severe qualitative failures, Fig. 1 shows a compilation of powder and single-crystal x-ray results from Ref. [30] up to 20 GPa. Two aspects of these data appear to be particularly remarkable. (i) On the one hand, the transition appears to be continuous within experimental resolution. Tentatively calculating the jumps that the lattice parameters would undergo according to the prediction (16b), we would obtain discontinuities $\Delta a = \Delta b \approx -0.014$ Å and $\Delta c = 0.048$ Å. Jumps of this magnitude are, however, clearly ruled out by experiment (cf. Fig. 1). Indeed, the second-order character of the transition at elevated pressure and the possibility of a tricritical point has already been noted some time ago in the classic Raman study Ref. [29]. Interestingly, such a change from first to second

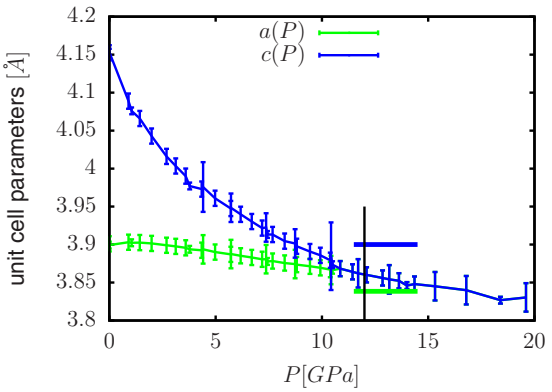

FIG. 1. Raw axis data for PTO obtained in Ref. [30] in the pressure range $0 \leqslant P \leqslant 20$ GPa. The value $P_c = 12$ GPa is indicated by the vertical line. The unobserved first-order jumps predicted from (16b) are marked by the two horizontal lines.

order character with increasing pressure is not only observed in the tetragonal-to-cubic transition of PTO but, for instance, also in that of KNO [32]. (ii) Equally puzzling is the observed curvature of the data that seems to increase as one lowers the pressure from P_c to ambient pressure. Given a second-order transition, the traditional Landau approach would predict a linear pressure dependence of the squared order parameter, inducing a similar P dependence of the spontaneous strain on top of the elastic background. In contrast, the observed behavior is neither expected nor explainable using standard Landau theory.

In summary, we observe serious inconsistencies between the traditional Landau approach and the experimental facts. Thus, it comes as no surprise that up to date we are not aware of any attempt to analyze these data further within the Landau framework. In what follows we shall demonstrate that our recently developed extension of Landau theory [10] allows us to carry out such an analysis successfully. However, the case of PTO turns out to pose some special challenges that may not be encountered in simpler applications of this theory. We therefore add a short discussion of the cornerstones of our flavor of Landau theory before we present its application to PTO in detail.

III. FINITE-STRAIN LANDAU THEORY

In a Landau-type approach, it is essential to recognize that a possible dependence on an external stress can be fully encoded in a double expansion of the Landau free energy $F(\boldsymbol{Q},\underline{\eta};\boldsymbol{X})$ in powers of the OP components Q_i and the components of the total strain tensor η_{ij} defined with respect to the zero-pressure ("lab") system $\boldsymbol{X}$. In previous literature, to capture strain effects beyond linear elasticity, some authors have tried to modify LPs of the above type by introducing P-dependent potential parameters in a more or less *ad hoc* manner. Frequently, this leads to "Landau potentials" in which both strains and stresses appear simultaneously. Such a strategy is neither mathematically consistent nor physically satisfying. Our present method strictly employs expansions in the strain components, even though our final results are parametrized by the underlying external pressure P, which nevertheless has always the status of a derived quantity, i.e., is a function of the applied strain. This is also very natural from the perspective of DFT.

Considering for simplicity the case of a scalar order parameter Q, in the laboratory system $\boldsymbol{X}_0$ such an expansion generally reads

$$\frac{F(Q,\underline{\eta};\boldsymbol{X}_0)}{V(\boldsymbol{X}_0)} \equiv \Phi(Q;\boldsymbol{X}_0) + \sum_{ijkl} \frac{C^{(2)}_{ijkl}[\boldsymbol{X}_0]}{2!}\eta_{ij}\eta_{kl} + \sum_{ijklmn} \frac{C^{(3)}_{ijklmn}[\boldsymbol{X}_0]}{3!}\eta_{ij}\eta_{kl}\eta_{mn} + \cdots + \sum_{N=1}^{\infty} Q^{2N} \sum_{ij} \eta_{ij}\left(D^{(2N,1)}_{ij}[\boldsymbol{X}_0] + \sum_{kl} \frac{D^{(2N,2)}_{ijkl}[\boldsymbol{X}_0]}{2!}\eta_{kl} + \sum_{klmn} \frac{D^{(2N,3)}_{ijklmn}[\boldsymbol{X}_0]}{3!}\eta_{kl}\eta_{mn} + \cdots \right), \tag{17}$$

where

$$\Phi(Q;\boldsymbol{X}_0) = \frac{A[\boldsymbol{X}_0]}{2}Q^2 + \frac{B[\boldsymbol{X}_0]}{4}Q^4 + \frac{C[\boldsymbol{X}_0]}{6}Q^6 + \cdots \tag{18}$$

denotes the "pure" OP contribution. Unfortunately, as it stands such an expansion is of very little use in practical applications. The presence of any strain powers beyond harmonic order results in a set of nonlinear coupled equilibrium equations which are extremely hard to handle. Furthermore, evaluating these powers would require knowledge of the numerical values of a rapidly increasing number of third, fourth, and higher order elastic constants $C^{(p)}_{ijklmn\ldots}[\boldsymbol{X}_0]$ as well as of the higher order coupling parameters $D^{(2N,p)}_{ijkl\ldots}[\boldsymbol{X}_0]$, neither of which are easily available in general. Consequently, the "traditional" attempts to apply Landau theory (LT) in a high-pressure context thus continue to regard η_{ij} as "infinitesimal" and truncate the above expansion at harmonic order in the strain. The terms ignored by such a crude approximation are precisely the ones that encode the nonlinear elastic effects inevitably accompanying high pressure. In cases where nonlinear effects are too obvious to be swept under the rug, the infinitesimal strain approach is therefore frequently augmented by *ad hoc* assumptions about an additional pressure dependence of elastic constants and strain-OP couplings that are difficult to justify.

On the other hand, one should realize that an expansion of type (17) actually contains much more information than needed. In fact, if we knew (17) to high orders, this would in principle allow us to compute the response of the system to an arbitrary external stress σ_{ij}. When only *hydrostatic external* stress is applied, however, all effects of elastic anisotropy necessarily originate solely from the emergence of a nonzero OP coupled to strain that effectively exerts a *nonhydrostatic*

internal stress. A much more economic approach should therefore exist for determining the response to hydrostatic external stress. Indeed, such a theory has recently been presented in Ref. [10] and was shown to yield a concise description of the ambient-temperature high-pressure phase transition in STO. We refer to Ref. [10] for a more detailed exposition of the machinery underlying FSLT. Here we content ourselves with summarizing its core ideas.

We start by emphasizing that "strain" is a relative concept. An expansion of a structure similar to (17) must therefore be possible also for another choice $\boldsymbol{X}_P$ of elastic reference system. To identify a particularly convenient "background" system, we argue that even though the total observed strain may be large, at least near P_c of a second-order or weakly first-order transition the spontaneous strain caused solely by emergence of nonzero equilibrium OP must necessarily be small enough to warrant a harmonic treatment. Thus we decompose the total strain $\eta_{ij} = \eta_{ij}(P)$ into

$$\eta_{ij} = e_{ij} + \alpha_{ki}\widehat{\epsilon}_{kl}\alpha_{lj}, \tag{19}$$

where α_{ik} denotes the deformation tensor [10] relating the zero-pressure ambient ("lab") system $\boldsymbol{X}_0$ to the chosen background system $\boldsymbol{X}_P$, which is therefore defined as the (hypothetical) equilibrium state of the system with the OP constrained to zero, and $e_{ik} = \frac{1}{2}(\sum_n \alpha_{ni}\alpha_{nk} - \delta_{ik})$ is the—possibly large—Lagrangian background strain. We emphasize that it is only with respect to the decomposition (19) that we are allowed to write

$$\frac{F(Q,\widehat{\underline{\epsilon}};\boldsymbol{X}_P)}{V[\boldsymbol{X}_P]} \approx \Phi(Q;\boldsymbol{X}_P) + Q^2 D_{ij}[\boldsymbol{X}_P]\widehat{\epsilon}_{ij} + \sum_{ij}\tau_{ij}[\boldsymbol{X}_P]\widehat{\epsilon}_{ij} + \frac{1}{2}\sum_{ijkl} C_{ijkl}[\boldsymbol{X}_P]\widehat{\epsilon}_{ij}\widehat{\epsilon}_{kl}. \tag{20}$$

For the pure OP potential part we assume

$$\Phi(Q;\boldsymbol{X}_P) = \frac{A[\boldsymbol{X}_P]}{2}Q^2 + \frac{B[\boldsymbol{X}_P]}{4}Q^4 + \frac{C[\boldsymbol{X}_P]}{6}Q^6 \tag{21}$$

with coefficients yet to be determined. As shown in Ref. [10], the OP equilibrium value $\bar{Q}$ minimizes a *renormalized background pure OP potential density*

$$\Phi_R(Q;\boldsymbol{X}_P) = \frac{A_R[\boldsymbol{X}_P]}{2}Q^2 + \frac{B_R[\boldsymbol{X}_P]}{4}Q^4 + \frac{C_R[\boldsymbol{X}_P]}{6}Q^6, \tag{22}$$

which is simply related to $\Phi(Q;\boldsymbol{X}_P)$ by

$$\Phi_R(Q;\boldsymbol{X}_P) = \Phi(Q;\boldsymbol{X}_P) - \frac{Q^2}{2}\sum_{ijkl} D_{ij}[\boldsymbol{X}_P]S_{ijkl} \times [\boldsymbol{X}_P]D_{kl}[\boldsymbol{X}_P], \tag{23}$$

where the compliance tensor $S_{mnij}[\boldsymbol{X}_P]$ is the tensorial inverse of the *Birch coefficients*

$$B_{ijkl}[\boldsymbol{X}_P] = C_{ijkl}[\boldsymbol{X}_P] + \tfrac{1}{2}(\tau_{jk}[\boldsymbol{X}_P]\delta_{il} + \tau_{ik}[\boldsymbol{X}_P]\delta_{jl} + \tau_{jl}[\boldsymbol{X}_P]\delta_{ik} + \tau_{il}[\boldsymbol{X}_P]\delta_{jk} - 2\tau_{ij}[\boldsymbol{X}_P]\delta_{kl}) \tag{24}$$

of the background system $\boldsymbol{X}_P$ which replace the elastic constants [36,37] at finite strain. A comparison of common powers in $\widehat{\epsilon}_{ij}$ yields the following expansions of the coefficients $A_R[\boldsymbol{X}_P], B_R[\boldsymbol{X}_P], C_R[\boldsymbol{X}_P]$, and $D_{ij}[\boldsymbol{X}_P]$ in powers of the background strain $e_{ij} = e_{ij}(P)$, with the laboratory couplings constituting (17) appearing as coefficients. One obtains

$$J D_{st}[\boldsymbol{X}_P] = \sum_{ij}\alpha_{si}D^{(2,1)}_{ij}[\boldsymbol{X}_0]\alpha_{tj} + \sum_{ijkl}\alpha_{si}D^{(2,2)}_{ijkl}[\boldsymbol{X}_0]\alpha_{tj}e_{kl} + \sum_{ijklmn}\alpha_{si}D^{(2,3)}_{ijklmn}[\boldsymbol{X}_0]\alpha_{tj}e_{kl}e_{mn} + \cdots, \tag{25}$$

$$J A_R[\boldsymbol{X}_P] = A[\boldsymbol{X}_0] + 2\Big(\sum_{ij}D^{(2,1)}_{ij}[\boldsymbol{X}_0]e_{ij} + \frac{1}{2!}\sum_{ijkl}D^{(2,2)}_{ijkl}[\boldsymbol{X}_0]e_{ij}e_{kl} + \frac{1}{3!}\sum_{ijklmn}D^{(2,3)}_{ijklmn} \times [\boldsymbol{X}_0]e_{ij}e_{kl}e_{mn} + \cdots\Big), \tag{26}$$

$$J B_R[\boldsymbol{X}_P] = B[\boldsymbol{X}_0] - 2J\sum_{ijkl}D_{ij}[\boldsymbol{X}_P]S_{ijkl}[\boldsymbol{X}_P]D_{kl}[\boldsymbol{X}_P], \tag{27}$$

$$J C_R[\boldsymbol{X}_P] = C[\boldsymbol{X}_0], \tag{28}$$

where $J := \det(\alpha_{il})$. Relation (25) indicates a pressure dependence of the strain-OP coupling constants resulting from nonlinear elastic effects, while (26) generalizes the linear pressure dependence of the harmonic Landau parameter familiar from the traditional infinitesimal strain approach. Relation (27), which is written in a compact way thanks to the previous relation (25) for $D_{kl}[\boldsymbol{X}_P]$, gives a pressure-dependent generalization of the constant negative renormalization of the fourth-order Landau parameter accompanying a linear-quadratic strain-OP coupling. Such a shift of the fourth-order coefficient is familiar from infinitesimal-strain Landau theory, where it is discussed as a possible mechanism for explaining the appearance of tricritical or first-order behavior. However, it is crucial to note that within the simple linearized theory no fully consistent explanation of an observed *pressure-dependent* change of the order of transition (second order, tricritical, first order) based on this device can be given. Finally, according to (28) the sixth-order Landau parameter acquires only a trivial renormalization with the current assumptions made.

Superficially, the equilibrium value $\widehat{\bar{\epsilon}}_{mn}$ of the spontaneous strain

$$\widehat{\bar{\epsilon}}_{mn} = -\bar{Q}^2\sum_{ij}D_{ij}(\boldsymbol{X}_P)S_{mnij}[\boldsymbol{X}_P] \tag{29}$$

still seems to follow the traditional Landau rule of thumb that for linear-quadratic coupling the spontaneous strain is proportional to the square of the OP. However, while the accompanying proportionality factor represents a mere constant in the infinitesimal approach, relation (29) indicates that this factor must be expected to become pressure-dependent in a nontrivial way as a result of the interplay between the pressure-dependent elastic constants and coupling constants in the nonlinear regime.

For an application to PTO we specialize equations (26) and (25) to a cubic background reference system $\boldsymbol{X}_P$. Then $J = V(P)/V(0)$, which yields a diagonal deformation tensor $\alpha_{ij} \equiv \alpha\delta_{ij}$ with $\alpha = \sqrt[3]{J}$ and a diagonal Lagrangian background strain $e_{ij} \equiv e\delta_{ij}$ with $e = \frac{1}{2}(\alpha^2 - 1)$. While this specialization leaves (27) and (28) unchanged, Eqs. (25) and (26) simplify to

$$\alpha(P)D_\mu[\boldsymbol{X}_P] = D_\mu[\boldsymbol{X}_0] + e(P)E_\mu[\boldsymbol{X}_0] + e^2(P)F_\mu[\boldsymbol{X}_0] + e^3(P)G_\mu[\boldsymbol{X}_0] + \cdots, \quad \mu = 1,2,3, \tag{30}$$

$$\alpha^3(P)A_R[\boldsymbol{X}_P] = A[\boldsymbol{X}_0] + 2\Big(e(P)D[\boldsymbol{X}_0] + \frac{e^2(P)}{2!}E[\boldsymbol{X}_0] + \frac{e^3(P)}{3!}F[\boldsymbol{X}_0] + \frac{e^4(P)}{4!}G[\boldsymbol{X}_0] + \cdots\Big) + \cdots, \tag{31}$$

where we introduced the abbreviations

$$D_\mu[\boldsymbol{X}] := D^{(2,1)}_\mu[\boldsymbol{X}], \quad E_\mu[\boldsymbol{X}] := \sum_\nu D^{(2,2)}_{\mu\nu}[\boldsymbol{X}],$$
$$F_\mu[\boldsymbol{X}] := \sum_{\nu\sigma} D^{(2,3)}_{\mu\nu\sigma}[\boldsymbol{X}], \quad G_\mu[\boldsymbol{X}] := \sum_{\nu\sigma\tau} D^{(2,4)}_{\mu\nu\sigma\tau}[\boldsymbol{X}], \quad \ldots \tag{32}$$

and

$$D[\boldsymbol{X}] := \sum_\mu D_\mu[\boldsymbol{X}], \qquad E[\boldsymbol{X}] := \sum_\mu E_\mu[\boldsymbol{X}],$$
$$F[\boldsymbol{X}] := \sum_\mu F_\mu[\boldsymbol{X}], \qquad G[\boldsymbol{X}] := \sum_\mu G_\mu[\boldsymbol{X}], \quad \ldots. \tag{33}$$

FSLT is constructed to serve as a high-pressure extension of an existing ambient-pressure LT. The minimal required input of FSLT for a successful application in this respect consists of the following ingredients:

(1) A preexisting ambient-pressure LT, supplying the laboratory coefficients $A[\boldsymbol{X}_0], B[\boldsymbol{X}_0], C[\boldsymbol{X}_0], D^{(2,1)}_\mu[\boldsymbol{X}_0] \equiv D_\mu[\boldsymbol{X}_0]$ and possibly ambient-pressure elastic constants $C_{\mu\nu}[\boldsymbol{X}_0]$. Obviously, such a LT constitutes a "boundary condition" that any high-pressure extension must meet. Our theory fulfills this requirement by construction, since $\boldsymbol{X}_P = \boldsymbol{X}_0$ implies $\alpha_{ij} = \delta_{ij}$ and thus $e_{ij} = 0$.

(2) The pressure dependence $e_{ij} = e_{ij}(P)$, i.e., $\alpha_{ij} = \alpha_{ij}(P)$, defining the "floating" reference system $\boldsymbol{X}_P$ must be known. If the high-symmetry phase is cubic, as it is in the present case, this amounts to knowledge of the equation of state (EOS) $V = V(P)$ from experiment or *ab initio* simulations.

(3) Similarly, we rely on knowledge of the pressure-dependent elastic constants $C_{ijkl}[\boldsymbol{X}_P] \equiv C_{ijkl}(P)$, constituting a relatively small set of P-dependent functions that encode the effects of higher order elastic constants at purely hydrostatic stress in a way that is much easier to handle. Unfortunately, experimental high-pressure measurements of pressure-dependent elastic constants are only available in rare cases. While in a precursor to our present theory [38] this P dependence had to be encoded in an expansion in powers of P constrained only by consistency with the pressure-dependent bulk modulus $K(P)$, which gave rise to additional fit parameters, in the present version pressure-dependent elastic constants are calculated from DFT.

Given these additional data, the only remaining free parameters are the higher order coupling coefficients $D^{(2,2)}_{ijkl}[\boldsymbol{X}_0], D^{(2,3)}_{ijklmn}[\boldsymbol{X}_0], \ldots$ appearing in the ambient pressure LP (17). Theoretically it could be possible to actually determine these coefficients (as well as higher order elastic constant components) from some sophisticated simulation or experiment. In practice, however, it is probably fair to say that in a genuine application of FSLT these couplings must be taken as unknown parameters to be determined from fitting the predictions of the theory to a set of experimental measurements. This may sound disturbing, since in a low-symmetry situation the number of independent components constituting these tensors can be quite substantial. However, in cases where the "high symmetry" paraphase—defined by the requirement that the OP vanishes identically—is, e.g., of cubic symmetry, Eqs. (30) and (31) indicate that only certain *sums* of these coefficients actually enter into our expansions. Thus, if the background system is highly symmetric, the actual number of independent free parameters is drastically reduced. For instance, Eqs. (30) and (31) reveal that to describe a cubic-to-tetragonal transition one needs to determine only two free parameters at each order in the background strain e. In situations of lower symmetry we may find ourselves in a less favorable situation. Unfortunately, however, there seems to be no consistent way of simplifying the problem any further without sacrificing key elements of nonlinear elasticity.

The theory we have summarized so far was developed in Ref. [10] to describe the high-pressure extension of the 105 K transition $Pm\bar{3}m \leftrightarrow I4/mcm$ in STO. In particular, it assumes that the low-pressure phase coincides with the high-symmetry parent phase. For the ferroelectric transition in PTO, however, this aspect seems to be reversed. The ambient temperature and pressure phase $P4mm$ of PTO is ferroelectric, and the transition to the cubic $Pm\bar{3}m$ reference phase mediated by a soft mode at the Γ point [29] heuristically conforms to the rule of thumb that pressure tends to suppress ferroelectricity [39] at least up to some critical pressure [40,41]. From the point of view of traditional LT, this difference, which also manifests itself in the different sign of the Clapeyron slopes dP_c/dT computed for both transitions, seems to be merely related to the signs of the OP-strain coupling constants. However, in setting up a FSLT extension, some extra care is needed. This becomes obvious if one takes into account that at ambient pressure and temperature the background strain $\boldsymbol{e}$ vanishes by definition if measured with respect to the laboratory state $\boldsymbol{X}_0$, which in turn implies that the total strain $\underline{\eta} = \underline{\epsilon}$ is all spontaneous. This state of affairs seems to thwart our plans developed above, which explicitly rest on the assumption that $\underline{\epsilon}$ would be small and $\boldsymbol{e}$ large. A remedy is, of course, to trade the $\boldsymbol{X}_0$ for a different reference system $\boldsymbol{X}_{P_r} \equiv \boldsymbol{X}_r$ defined for some pressure $P_r > P_c$, which is always possible, since strain, as we once more emphasize, is a relative concept. The resulting slight technical complications in applying FSLT are described in Appendix A.

IV. FINITE TEMPERATURE

For notational reasons we have suppressed an additional temperature dependence of the constituents entering the theory sketched above. Assuming that the T dependence of the

ambient-pressure LP is known, this still leaves us with determining that of all remaining coupling parameters defined with respect to the background reference system $\boldsymbol{X}_R$. In particular, we should find a way to "heat up" the EOS and pressure-dependent elastic constants that we have obtained from DFT to the desired temperature. If one studies a transition at rather low temperatures one may try to get away with ignoring effects related to finite temperature such as thermal expansion or temperature changes in the elastic constants in a first approximation. This applies, e.g., to the cubic-to-tetragonal transition of STO used as a test bed for FSLT in Ref. [10], which takes place at a modest $T_c = 105$ K. In the case of PTO, neglecting finite-temperature effects would be much harder to justify, since the ambient-pressure ferroelectric transition takes place at the rather elevated temperature of $T_c \approx 765$ K.

Some time ago, a very interesting and ambitious strategy to obtain finite-temperature results from DFT has been worked out [42–47] with the declared objective to obtain a parameter-free description. It consists of (i) isolating those unstable deformation modes that initiate the symmetry breaking accompanying the transition, (ii) calculating an effective lattice Hamiltonian for these modes, including couplings to further important deformations such as lattice strain, and (iii) feeding this into Monte Carlo [46] or molecular dynamics [48]. This approach has indeed offered remarkable qualitative and semiquantitative insight into the mechanisms underlying, e.g., structural phase transitions. In addition, it also shares a lot of common ground with Landau theory due to its strong emphasis of group theory. However, the effective Hamiltonian approach typically fails to reproduce the experimentally observed critical temperatures in perovskites, sometimes by several tens of kelvins or more. In Ref. [49] these problems were traced back to an insufficient incorporation of noncritical anharmonic effects.

Our present approach does not aim at calculating coupling parameters of energy contributions involving the OP. It only requires determining the dependence of the background system $\boldsymbol{X}_P$ on P and T for zero OP. However, $\boldsymbol{X}_P$ is—by definition—*thermodynamically unstable* within the broken-symmetry phase, and therefore it is not straightforward how to determine the T dependence of the EOS and elastic constants of the high-symmetry reference phase. Of course, this problem is not at all specific to high-pressure situations (in the context of effective Hamiltonians cf. Ref. [42]). Indeed, it should arise any time that a secondary OP (i.e., a tensorial quantity that does not break as many symmetry elements as the primary OP when assuming a nonzero value [50]) is included in LT. To disentangle the transition anomalies related to such a secondary OP from possible noncritical contributions, some potentially T-dependent "baseline" always needs to be subtracted. Drawing such a thermal "base line" to disentangle transition-related anomalies of a secondary order parameter from some background not related to broken symmetry may be considered a trivial matter. However, it is not. In the ferroelectric literature, elastic baselines have been defined at ambient pressure in various ways. For instance, Ref. [22] explicitly defines a pseudocubic unit cell parameter as the third root of the noncubic unit cell volume, whereas conveniently imposing the condition of T independence for the coupling parameters between strain and polarization [23] constitutes an implicit one. Of course, the fitted Landau parameters emerging from such an *ad hoc* prescription inherit a similar degree of arbitrariness. Moreover, the resulting elastic baseline is likely to be incompatible with one obtained from a thermal extension of an EOS calculated from DFT. While these issues may remain unnoticed at modest pressures, they are bound to surface in an attempt to construct FSLT as the high-pressure extension of this LP.

For solid state systems, a standard way of passing from energies to free energies is the quasiharmonic approximation (QHA) [36,51–53]. In principle the QHA requires computing the zero-temperature phonon frequencies at any given volume of the high-symmetry phase which is well mastered by DFT. By definition, however, the high-symmetry reference structure of a structurally unstable system will exhibit at least one unstable phonon mode characterized by an imaginary frequency. In the lattice-dynamical description of structural phase transitions this imaginary frequency corresponds to the "soft mode" that becomes unstable at the transition. Indeed, the phonon dispersions calculated for typical perovskites generally feature several rather "flat" branches of imaginary modes stretching into extended regions of the Brillouin zone (see, e.g., the phonon dispersion graphs on p. 135 of Ref. [13]). The corresponding large spikes in the phonon density of states (DOS) $g(\omega)$ make it impossible to simply neglect these phonon branches. It is due to the presence of these imaginary phonons that standard techniques for incorporating thermal effects such as the quasiharmonic approximation (QHA) and Grüneisen theory [54,55] cannot be applied. Ways to overcome the fundamental difficulties posed by the presence of imaginary phonon modes and strong anharmonicity continue to constitute an active area of current research (see, e.g., Refs. [56,57]).

The nonapplicability of the QHA is a recurrent theme in high-pressure and mineral physics even in the absence of imaginary phonons simply because precise information on the phonon DOS is frequently unavailable due to the complexity of the corresponding systems. In these fields different types of Debye approximations (DAs) are therefore still essential [58–61]. As we recall in Appendix C, where we recollect the most relevant facts of the DA in the present context for the reader's convenience, the simplest forms of the DA require only knowledge of the underlying EOS and a rough guess of the Poisson ratio σ. It is these modest requirements that make the Slater-Debye approximation equally appealing in our present situation, in which the phonon DOS of the high-symmetry structure is available but nevertheless unusable due to the imaginary frequency contributions.

A general solution of the issues raised by the presence of an imaginary contribution to the phonon spectrum must be postponed to future work. For now, our proposed strategy for determining the finite-temperature dependence of a (e.g., cubic) high-symmetry reference structure consists of performing constrained DFT calculations of the corresponding cubic EOS and elastic constants followed by a subsequent application of the DA. In view of the rather drastic simplifications implied by such strategy, we shall take a pragmatic point of view with respect to the choice of DA flavor described above. In a typical problem at hand, we may have experimental volume data at several temperatures available, and we shall choose

the combination of DFT and DA type that exhibits the most satisfactory overall agreement with the available data.

We close this section with some practical advice. A generic application of this theory will typically involve fitting a set of P-dependent strain data, for which rather precise additional information on the actual value of the critical pressure P_c may frequently be available. By its very nature, a least-squares fitting procedure may however numerically trade a better fit to data points far away from the transition for a shift of P_c to some other value. To avoid such a numerical smearing of the transition pressure region, we recommend numerically eliminating one of the free fit parameters, say $E_1[\boldsymbol{X}_0]$, in favor of P_c. Provided we are dealing with a second-order transition, this can be accomplished, for example, by solving the equation $A_R[\boldsymbol{X}_{P_c}] \equiv 0$ for $E_1[\boldsymbol{X}_0]$.

V. APPLICATION TO LEAD TITANATE

The above discussion has underlined that a prerequisite for a successful description of the ambient-temperature high-pressure phase transition in lead titanate reported in Ref. [30] is the determination of a meaningful background system $\boldsymbol{X}_P$ at a given temperature T. This amounts to calculating the EOS $V = V(P,T)$ and the elastic constants $C_{11}(P,T)$,$C_{12}(P,T)$ for the cubically constrained system. At $T = 0$ we accomplish this task by performing a series of standard DFT calculations. Details are deferred to Appendix B.

The behavior of the resulting elastic baselines at finite temperature and pressure is analyzed using the GIBBS2 package [52,53]. Further details can be found in Appendix C. As stated above, we take a pragmatic point of view and try to single out the type of DA that yields the best overall agreement of the thermally extrapolated cubic EOS $V = V(P,T)$ with the available data. On the one hand, at ambient pressure, this function should reproduce the one of Haun *et al.* [23] for $T > T_c$. On the other hand, at room temperature it should match the volume data of Janolin *et al.* [30] for 12 GPa $\leqslant P \leqslant$ 20 GPa. In addition, between 0 and 7.8 GPa high-temperature cubic EOSs have been measured rather recently using synchrotron x-ray diffraction by Zhu *et al.* [33] at temperatures $T =$ 674 K, 874 K, and 1074 K. Unfortunately, no matter which type of the DAs implemented in GIBBS2 was invoked, it proved to be impossible to perfectly match these requirements simultaneously.

In detail, the Dugdale-McDonald and Vaschenko-Zubarev flavors of Debye-Grueneisen approximations (see Appendix C) admittedly produced the best-fitting baseline to the volume data of Janolin *et al.* Also, they yielded good agreement with those of Zhu *et al.* However, these approximations produced a certain small but non-negligible offset to the $T > T_c$ part of the baseline of Haun *et al.* Concise agreement with the high-temperature part of this baseline must, however, be regarded as an important constraint in our search, since our set of Landau coefficients is directly based on these data.

Interestingly, the simple DA is not only found to perform excellent in this respect (Fig. 2), but also to produce an ambient-temperature baseline for the high-temperature volume data that is in reasonable agreement with the volume data of Janolin *et al.* between 12 and 20 GPa (cf. Fig. 2), which is an indispensable prerequisite for application of our FSLT.

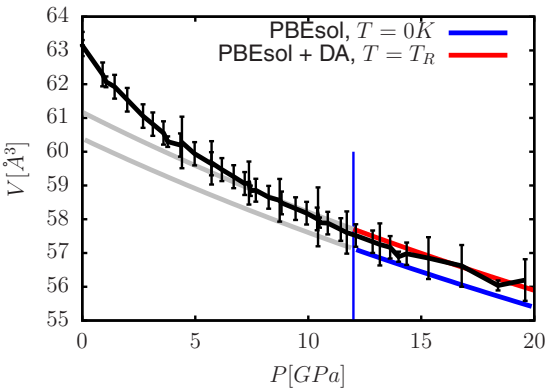

FIG. 2. Comparison of raw volume data of Janolin *et al.* [30] (black line) to the thermal EOS derived from the PBEsol functional and the DA (red line). To illustrate the effect of thermal expansion, the EOS resulting from zero-temperature DFT is also shown (blue line).

The values obtained from the simple DA are, however, in excess of the synchrotron data of Zhu *et al.* by some 3.5%. The reason for the discrepancy is currently not understood. It may very well result from the intrinsic imperfections of the DA (as well as those of the QHA) at high temperatures. On the other hand, Zhu *et al.* also report certain disagreements of the accompanying values they obtained for the bulk modulus with those previously obtained by other authors.

In summary, for our present purposes a combination of PBEsol and a simple DA emerged as a reasonable choice for producing a suitable T- and P-dependent EOS. Based on the strategy outlined in Appendix C, this also allows us to extend the pressure-dependent elastic constants obtained from DFT from zero to finite temperature.

Looking at Fig. 3, one notices that upon lowering the temperature from T_c down to T_R our new baseline steadily deviates from the one of Haun *et al.*, and the spontaneous strain components emerging from these data have to be redefined with respect to this new baseline. This, in turn, requires revising the

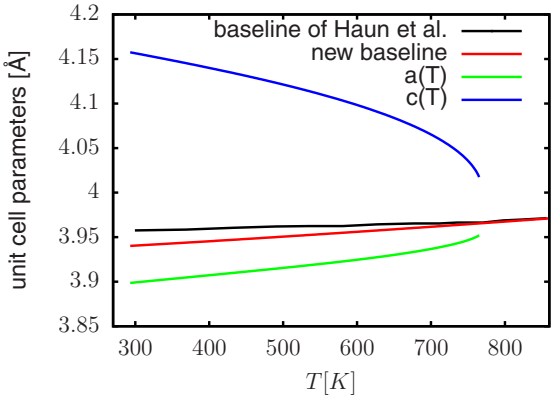

FIG. 3. Comparison of elastic baseline used in Haun *et al.* [23] (black) to our new baseline (red) as obtained from the Debye approximation. The temperature-dependent ambient pressure unit cell parameters $a(T)$ (green) and $c(T)$ (blue) are also shown for convenience.

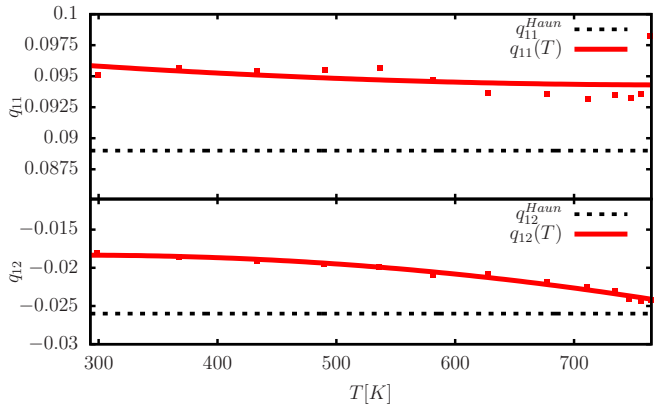

FIG. 4. Comparison of the T-independent coupling coefficients values $\widehat{q}_{ij}$ obtained by Haun *et al.* (black horizontal dashed lines; cf. Table I) to those obtained from redefining the elastic baseline using PBEsol and the DA [red data points, fitted by Eqs. (D1) (red line)].

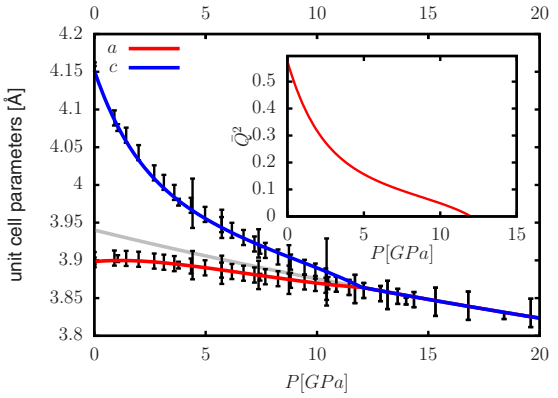

FIG. 6. Main plot: Fit of FSLT to experimental lattice parameters. The vertical line indicates the critical pressure $P_c = 12$ GPa. The gray line indicates the elastic thermal background reference system resulting from the use of PBEsol and the simple DA. Inset: Resulting P dependence of squared equilibrium OP.

values of the T-independent coupling coefficients $\widehat{q}_\mu$ of Haun *et al.* As demonstrated in Appendix D, one obtains a new set of somewhat shifted and slightly T-dependent coupling coefficients $\widehat{q}_\mu = \widehat{q}_\mu(T)$. In principle, the thereby acquired T dependence may still appear rather weak (cf. Fig. 4) and could very well be neglected. More importantly, however, Fig. 4 reveals that the overall levels of the couplings have also undergone certain small but definitely non-negligible shifts. These readjustments of the OP-strain coupling parameters may appear small. Nevertheless, in retrospect they proved to be crucial for obtaining a good fit of FSLT to the high-pressure transition data.

Once the thermal baseline and a redefined set of strain-OP couplings have been established, we can extract (Lagrangian [36]) spontaneous strain components from the raw data of Janolin *et al.* The results, which are shown in Fig. 5, reveal that any discontinuous behavior of these components with respect to variations in the pressure cannot virtually exceed the size of the error bars, and certainly must be at least much smaller than the first-order discontinuities observed in the corresponding spontaneous strain components at the critical temperature of the ambient-pressure ferroelectric transition. This supports our initial hypothesis that the high-pressure transition at room temperature exhibits a second-order character. In contrast, Eq. (16b) derived from traditional LT predicts discontinuous jumps of the spontaneous strains with sizes independent of both T and P, that are clearly not observed.

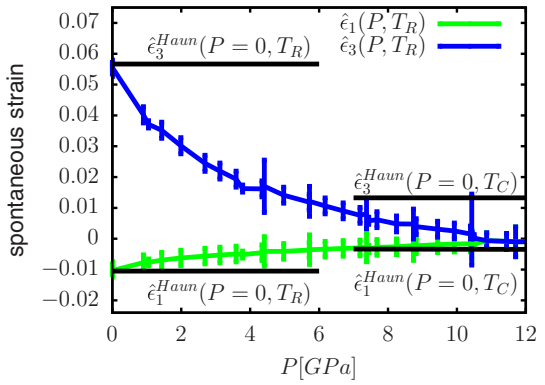

FIG. 5. Spontaneous Lagrangian strain components computed from the raw data of Janolin *et al.* [30] (shown in Fig. 1) after implementation of our new baseline at $T = T_R$. The corresponding spontaneous strains $\widehat{\epsilon}_\mu(T_R)$ and the critical jumps $\widehat{\epsilon}_\mu(T_C)$ of the ambient-pressure ferroelectric transition are also indicated.

With the above preparations completed, setting up the least-squares fit is rather straightforward. In detail, we placed our background reference system $\boldsymbol{X}_r$ at $P_r = 20$ GPa. As explained above, fixing $P_c = 12$ GPa allows us to eliminate $E_3[\boldsymbol{X}_r]$ from the list of free parameters, which thus reads $E_3[\boldsymbol{X}_r], F_1[\boldsymbol{X}_r], F_3[\boldsymbol{X}_r], G_1[\boldsymbol{X}_r], G_3[\boldsymbol{X}_r]$. In a simultaneous fit of the two data sets for the total strains $\eta_1(P)$ and $\eta_3(P)$ all of these parameters are initially put to zero.

The resulting fits to the experimental unit cell parameters a, c and the accompanying pressure dependence of the squared equilibrium OP $\bar{Q}^2(P)$ are shown in Fig. 6. In the inset to this figure, one immediately notices the strong deviation of $\bar{Q}^2(P)$ from the generally assumed linear P dependence predicted by infinitesimal-strain LT. Via Eq. (29), this pronounced nonlinearity is passed on to the unit cell parameters a and c, precisely producing the unusual curvatures of $a(P)$ and $c(P)$ away from their common baseline, as the main plot of Fig. 6 shows. It is the combined effects of the P dependence of elastic constants and the nonlinear strain-OP coupling terms that have made it possible to understand the unusual effects of nonlinear elasticity reflected in these experimental data.

The resulting P dependence of A_R is roughly linear as expected from standard LT (left upper corner of Fig. 7). However, while it necessarily reduces to the corresponding ambient-temperature value of the potential of Haun *et al.* for $P = 0$, its slope as a function of pressure is markedly reduced due to the fact that our FSLT is able to take the P dependence of elastic constants properly into account. This immediately resolves the discrepancy between the experimentally observed critical pressure $P_c = 12$ GPa and the value $P_c = 2.9$ GPa predicted by the infinitesimal-strain approach, in which any pressure dependence of elastic constants had been implicitly neglected.

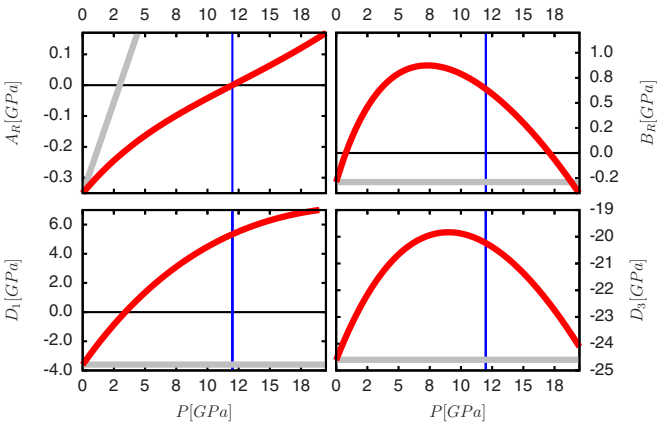

FIG. 7. P dependence of Landau coefficient A_R, B_R, D_1, D_3 at room temperature T_R (red lines). Vertical blue lines mark the critical pressure $P_c = 12$ GPa. For comparison, gray lines indicate the P dependence of the coefficients (7), (8), and (10) as computed from the Landau potential (2) of Haun *et al.*

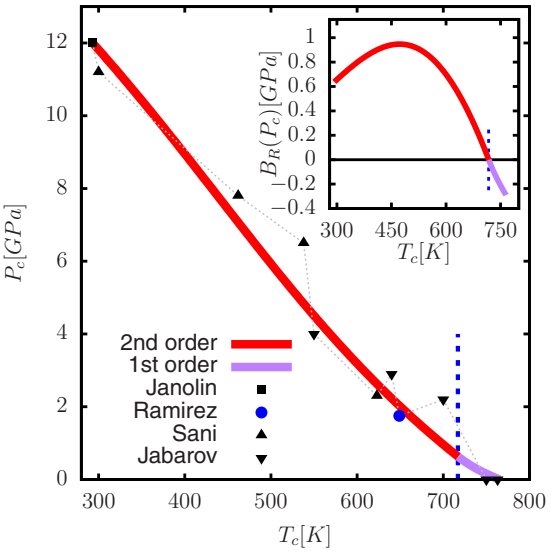

FIG. 8. Main plot: Comparison of tentative second-order (red line) and first-order (purple line) phase boundary $P_c = P_c(T_c)$ for $T_R \leqslant T \leqslant T_C$ as computed from our theory to literature values including the well-known ferroelectric transition at $T = T_c$ for which $P_C = 0$, the $P_c = 12$ GPa transition at $T = T_R$ measured by Janolin *et al.* [30]. The blue data point indicates the estimate of the tricritical point derived by Ramirez *et al.* in Ref. [64]. The remaining data points represent experimental results compiled from Refs. [65] and [66]. Inset: Values of B_R along the phase boundary. The tricritical temperature $T_{\text{tric}} \approx 717$ K derived from FSLT is indicated in both plots by the vertical dashed blue line.

Parameters D_μ show some P dependence, with D_1 remaining small in modulus and D_3 evolving in the range between -22 GPa and -19 GPa.

The P dependence of B_R is most interesting. In fact, it is the key to understanding the change of the character of the transition from first to second order with increasing pressure. For a scalar OP subject to a given LP, a second-order transition is expected for a positive sign of the quartic coupling constant $B > 0$. In contrast, for $B < 0$ a sixth-order term with a positive coupling constant $C > 0$ must be present in the LP for reasons of stability, and (since fluctuations are neglected [62]) standard LT always predicts a first-order transition [6]. In particular, the presence of a linear-quadratic coupling between OP and infinitesimal strain yields a negative renormalization [63] of the "bare" quartic OP coefficient B to a smaller value $B_R < B$ after the strain terms have been eliminated from the LP by using the elastic equilibrium conditions. In infinitesimal LT, this mechanism constitutes the standard theoretical quantitative device to explain the rule of thumb that strong elastic coupling is often accompanied by a first-order transition character. However, infinitesimal-strain LT only allows for a *P-independent* renormalization from B to B_R, while the observed change in transition character for PTO from first to second order with increasing P can only be due to a P-dependent change of sign of B_R, a behavior that is impossible to implement consistently in such an approach. In contrast, the coupling coefficient B_R resulting from FSLT naturally acquires a nontrivial P dependence, as immediately anticipated from a glance at Eq. (27). As displayed in the right upper corner of Fig. 7, B_R indeed starts out negative at ambient pressure, but quickly changes its sign with increasing P. Thus, the observed P dependence of B_R provides the sought-after explanation of the change in order of the transition from first to second order. In principle, this should not come as a surprise, since our theory was just designed as an interpolation capable of describing both the first-order ambient-pressure transition as well as second-order transition at 12 GPa. However, we emphasize once more that a similar mechanism cannot consistently be introduced in a LT based on infinitesimal strain.

Varying both pressure and temperature, the combined dependence of A_R and B_R on (P,T) allows us to estimate the location of the tricritical point in the phase diagram, which is defined as the state on the cubic-tetragonal phase boundary that separates the line of first-order transitions from that of second-order ones. Indeed, for variable temperature T the location of $A_R(P,T) \equiv 0$ as a function of pressure defines the cubic-tetragonal phase boundary $P_c = P_c(T_c)$, provided that the corresponding value B_R is positive. Otherwise, as follows from standard Landau reasoning, the transition pressure must be located by numerically solving the equation $A_R(P,T) \equiv \frac{3B_R^2(T,P)}{16C_R(P,T)}$. The resulting tentative phase diagram for PTO in the pressure range $0 \leqslant P \leqslant 20$ GPa is shown in Fig. 8. As shown in the inset of Fig. 8, B_R indeed changes sign along the phase boundary, and we estimate the corresponding tricritical point to be

$$(T_{\text{tric}}, P_{\text{tric}}) \approx (717\ \text{K}, 0.64\ \text{GPa}). \tag{34}$$

In closing this section we note that upon further increasing the pressure B_R drops towards large negative values for $P > 18$ GPa after passing through a maximum at approximately 7.5 GPa. It is tempting to interpret this behavior as an indication of the instability of the cubic phase for high pressure experimentally observed in Ref. [30].

VI. DISCUSSION AND CONCLUSION

We have presented an in-depth discussion of the application of FSLT to the room-temperature high-pressure ferroelectric phase transition of PTO, for which the conventional Landau approach based on truncating the free energy expansion in the strain tensor components beyond harmonic contributions fails. In contrast, FSLT allows us to understand the peculiar behavior of the tetragonal unit cell parameters as functions of pressure, the change of the character of the transition from first to second order with increasing pressure, to predict the phase boundary separating the cubic and tetragonal phase in the (P,T) plane, and to localize the corresponding tricritical point. In this final section we would like to comment on several points.

(i) While Fig. 8 indicates that the cubic-tetragonal phase boundary derived from our theory is in reasonable agreement with experimental data from the literature, we note that the predicted location (34) of the tricritical point differs somewhat from previous estimates in the literature. In particular, Samara [67] estimates the tricritical pressure of PTO to be $P_{\text{tric}} \approx 4.5$ GPa by analyzing dielectric measurements, while Ramirez *et al.* [64] gather evidence for $(T_{\text{tric}}, P_{\text{tric}}) = (649\ \text{K}, 1.75\ \text{GPa})$. To understand these discrepancies, one has to take into account that dielectric measurements on pure PTO crystals are usually hampered by their large room conductivity resulting from lead deficiency. This problem is greatly reduced for slightly U^{5+}-doped single crystals [21], which had therefore been used for the measurements of Ref. [67], on which also the estimate of Ref. [64] was based. Unfortunately, as Ref. [8] reports, it later turned out that reproducibility of dielectric measurement results for different U-doped crystal specimens was not very reliable, with peak values of the dielectric constant at T_c varying by factors up to 3 and specific heat and slope dP_c/dT by factors up to 2.

(ii) From a pure *ab initio* perspective, our present approach cannot compete with the elaborate and parameter-free effective Hamiltonian method sketched in Sec. IV. Still, since it is not plagued by its lack of precision in determining T_c, it is able to offer much greater numerical accuracy in describing a given set of experimental data. This is only possible because the knowledge of a T-dependent LP at ambient pressure is already presupposed, and we merely construct a DFT-aided extension of this existing thermal theory from ambient to high pressure.

In passing, we note that even if we were in possession of a perfect microscopic effective Hamiltonian, it would still be far from trivial to determine the resulting temperature-dependent Landau parameters from Monte Carlo simulations (as shown in Refs. [68,69], one pitfall is the unavoidable occurrence of phase separation below T_c).

(iii) As we have shown, the construction of the finite-temperature extensions of the EOS and elastic constants of the cubic reference phase turned out to be an essential prerequisite for the successful description of the high-pressure transition of PTO and also enforced a redefinition of Landau parameters previously established in the literature. The main obstacle in determining this thermal extension is the presence of imaginary phonon modes indicating the low-temperature instability of this reference phase. It is important to realize that such problems are unavoidable in any attempt to combine LT with *ab initio* calculations. Electronic structure methods like DFT generally work at $T = 0$, whereas a high-symmetry (and thus, in general, high-temperature) reference state is pivotal to LT. In the present work, this difficulty was circumvented by employing a DA based on the EOS and elastic constants obtained from DFT, but a more fundamental and controlled solution of this problem, which might be based on, e.g., ideas of Refs. [56,70] or [71] is definitely welcome. Work in this direction is currently in progress.

(iv) We certainly do not want to leave the impression that our work is the only one that accounts for the effects of nonlinear elasticity and large strains at structural phase transformations. For instance, the last decade has witnessed considerable progress in the description of strong first-order martensitic phase transformations in shape memory alloys and steels (see, e.g., Refs. [72–77] and references therein). For the construction of the corresponding phase field models a finite-strain treatment turns out to be mandatory. However, strong martensitic transformations are not of the standard group-subgroup type, but rather fall under the class of reconstructive transitions [78], for which it is impossible to define an OP in the strict sense of orthodox LT (i.e., based on a single irreducible representation of a high-symmetry reference group). Accordingly, the mechanism of these martensitic transitions is not related to a particular phonon instability; i.e., the soft-mode picture does not apply.

ACKNOWLEDGMENTS

A.T. is grateful to A. Otero-de-la-Roza for advice using the GIBBS2 program package. A.T. and K.B. acknowledge support by the Austrian Science Fund (FWF) Project No. P27738-N28. S.E. acknowledges support from HEC, Pakistan, and would like to thank F. Tran for help with the DFT calculations. S.E. and P.B. acknowledge support from FWF SFB F41 (ViCom). J.K. acknowledges support from the Fonds National de la Recherche, Luxembourg, through a Pearl grant (FNR/P12/4853155/Kreisel). W.S. acknowledges support by the Austrian Science Fund (FWF) Project No. P28672-N36.

APPENDIX A: BROKEN SYMMETRY AT HIGH VS LOW PRESSURE

The success of the strategy of FSLT as outlined in Sec. III hinges on (i) knowledge of the LP as defined with respect to the ambient pressure reference system $\boldsymbol{X}_0$, (ii) the possibility to split the total strain into a spontaneous contribution $\widehat{\epsilon}_{ij}$ assumed small enough to warrant harmonic treatment for a second-order transition close to P_c, and a "large" background strain e taking care of all pressure effects that are unrelated to the primary OP. Equating coefficients of a power series in $\widehat{\epsilon}_{ij}$ allowed us then to calculate the pressure dependence of Landau parameters. For STO, this strategy worked great. For the "upside-down" case of PTO the decomposition of total strain into background and spontaneous part may still be useful around P_c, but it fails exactly where we need it the most: at ambient pressure. Relative to the zero-pressure reference

system $\boldsymbol{X}_0$, the background strain must vanish, and the total strain is all spontaneous. With every coefficient vanishing, it makes also no sense to equate common powers of $\widehat{\epsilon}_{ij}$.

An obvious solution to the described "upside-down" situation would be to choose another reference system $\boldsymbol{X}_r$. If one tries to mirror the case of STO, the state at a reference pressure $P_r \equiv 20$ GPa appears to be a logical choice. The drawback is, of course, that the parameters of the initial LT are still given with respect to the laboratory system $\boldsymbol{X}_0$. We therefore have to transfer these values first to the new reference system $\boldsymbol{X}_r$ before we can employ them in a thereby slightly generalized version of FSLT. To construct this theory, one notices that the basic strategy of imposing invariance of the description under a change of elastic reference frame and the strategy of comparing common powers of the spontaneous strain components remain intact under such a generalization. In terms of

$$j_r(P) = \frac{V(P)}{V(P_r)}, \quad \alpha_r(P) = j_r^{1/3}(P), \quad e_r(P) = \frac{1}{2}\left[\alpha_r^2(P) - 1\right], \tag{A1}$$

we now find

$$\alpha_r(P) D_\mu[\boldsymbol{X}_P] = D_\mu[\boldsymbol{X}_r] + e_r(P) E_\mu[\boldsymbol{X}_r] + e_r^2(P) F_\mu[\boldsymbol{X}_r] + e_r^3(P) G_\mu[\boldsymbol{X}_r] + \cdots, \quad \mu = 1,2,3, \tag{A2}$$

$$\alpha_r^3(P) A_R[\boldsymbol{X}_P] = A[\boldsymbol{X}_r] + 2\left(e_r(P) D[\boldsymbol{X}_r] + \frac{e_r^2(P)}{2!} E[\boldsymbol{X}_r] + \frac{e_r^3(P)}{3!} F[\boldsymbol{X}_r] + \frac{e_r^4(P)}{4!} G[\boldsymbol{X}_r] + \cdots\right) + \cdots. \tag{A3}$$

It remains to transfer our knowledge of the ambient-pressure LP parameters to the new reference system $\boldsymbol{X}_r$. Specializing to $P = 0$, one gets

$$D_\mu[\boldsymbol{X}_r] = \alpha_r(0) D_\mu[\boldsymbol{X}_0] - e_r(0) E_\mu[\boldsymbol{X}_r] + e_r^2(0) F_\mu[\boldsymbol{X}_r] + e_r^3(0) G_\mu[\boldsymbol{X}_r] + \cdots, \quad \mu = 1,2,3. \tag{A4}$$

This also carries over to the other couplings. For instance, in terms of the sums (33) we similarly obtain

$$A[\boldsymbol{X}_r] = \alpha_r^3(0) A_R[\boldsymbol{X}_0] - 2\left(e_r(0) D[\boldsymbol{X}_r] + \frac{e_r^2(0)}{2!} E[\boldsymbol{X}_r] + \frac{e_r^3(0)}{3!} F[\boldsymbol{X}_r] + \frac{e_r^4(0)}{4!} G[\boldsymbol{X}_r] + \cdots\right) + \cdots. \tag{A5}$$

In this way, we are retaining the information about the $\boldsymbol{X}_0$ couplings constituting the ambient-pressure LT, while trading the—usually unknown—quantities $E_\mu[\boldsymbol{X}_0], F_\mu[\boldsymbol{X}_0], G_\mu[\boldsymbol{X}_0], \ldots$ for the equally unknowns $E_\mu[\boldsymbol{X}_r], F_\mu[\boldsymbol{X}_r], G_\mu[\boldsymbol{X}_r], \ldots$, which thus serve as yet another set of fit parameters in a practical application.

APPENDIX B: DFT CALCULATION OF EOS AND ELASTIC CONSTANTS

The EOS and elastic constants of the cubic phase were performed using the WIEN2K DFT package [81], an all-electron code including relativistic effects. WIEN2K is based on the full-potential (linearized) augmented plane-wave ((L)APW) + local orbitals (lo) method [82], one among the most accurate schemes for band structure calculations. For the present calculation, an APW + lo type basis set was employed. Its size, which is the main parameter governing the quality of convergence of a given simulation, depends on the product $R_{\mathrm{MT}}^{\mathrm{min}} \times K_{\mathrm{max}}$, where $R_{\mathrm{MT}}^{\mathrm{min}}$ is the smallest muffin tin radius in the unit cell and K_{max} is the largest reciprocal lattice vector considered. Using muffin-tin radii of $R_{\mathrm{MT}} = 2.1$ bohrs, 1.77 bohrs, and 1.6 bohrs for lead, titanium, and oxygen, respectively, the safe choice [82] $R_{\mathrm{MT}}^{\mathrm{min}} \times K_{\mathrm{max}} \equiv 8$ produces $K_{\mathrm{max}} = 5\,\mathrm{bohr}^{-1}$. For total energy calculations a $10 \times 10 \times 10$ k mesh in the Brillouin zone turned out to be sufficient to establish convergence.

As to the choice of XC functional, it is worth mentioning that the well-documented inadequacy [83] of both LDA and PBE functionals in application to ferroelectric perovskites is particularly severe for the tetragonal phase of PTO. In fact, this very issue has played an important role in the improvement of GGA functionals for applications to solids [84–86]. While we have also explored standard LDA as well as PBE [87,88] functionals, we can confirm previous observations [10,89] according to which for perovskites the Wu-Cohen [84] and PBEsol functionals [85] give overall satisfying agreement with experiment. In passing we mention that we have also included spin-orbit coupling to account for the relativistic effects due to the presence of lead. However, not unexpectedly the corresponding effects turned out to be rather small.

Our procedure to determine the behavior of the background system $\boldsymbol{X}_P$ starts by computing the total energy per unit cell for a number of different volumes roughly covering the expected pressure range between 0 and 20 GPa. A standard third-order Birch-Murnaghan EOS [90] is found to allow for an excellent fit to these data. For the choice of PBEsol, on which we shall focus from now on, it produces the zero-temperature EOS parameters $V_0 = 60.388\,\mathrm{bohr}^3$, $K_0 = 190.7$ GPa, and $K_0' = 4.5$. Armed with this zero-temperature EOS $V = V(P)$, we determined the cubic zero temperature elastic constants $C_{ij}(P)$ by performing a systematic series of hydrostatic, uniaxial, and rhombohedral deformations, fitting the resulting energy curves to polynomials, and extracting the corresponding curvatures at the minimum. Within the WIEN2K environment, this task is in principle conveniently performed using the corresponding package by Charpin [81]. Results are shown in Fig. 9.

Table II provides a comparison of our all-electron results for the ambient pressure cubic phase of PTO to previous ones from the literature. In particular, it should serve to warn nonspecialists of DFT not to expect different DFT codes to yield identical results even if the corresponding calculations are based on

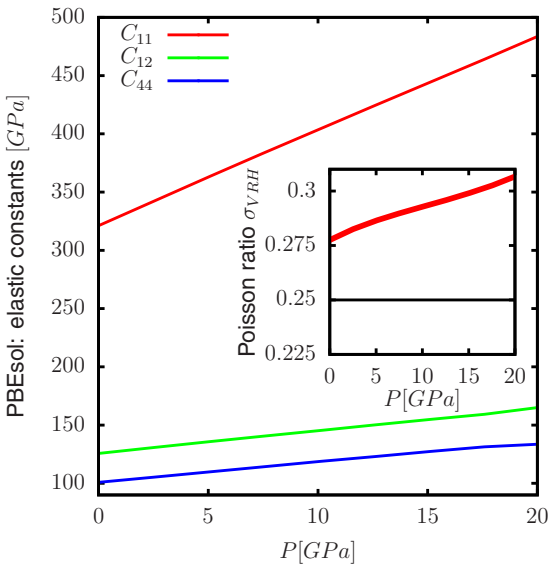

FIG. 9. Main plot: Pressure dependence of zero-temperature elastic constants of PTO as obtained from DFT using the PBEsol functional. Inset: P dependence of Poisson ratio as computed from Eq. (C4). The default value $\sigma = 1/4$ used in the GIBBS2 package, which corresponds to a Cauchy solid, is also indicated as a guide to the eye.

the same choice of XC functional. In practice the quality of the obtained results may depend significantly on various other ingredients such as the type of pseudopotential used, the basis set employed, the number of k-mesh points, and so on. For instance, the tendency of LDA to produce overbinding is well known [91]. Therefore, the fact that the lattice constant $a_0 = 4.09$ Å obtained in Ref. [80] from an LDA calculation appears to be larger than all other corresponding values in Table II should raise severe doubts on the validity of the elastic constants reported in this reference as well. But Table II also reveals that even if two calculations show nice agreement of the equilibrium lattice parameters and bulk moduli, that does not necessarily guarantee that the corresponding elastic constants derived from these calculations do so. In summary, keeping in mind that elastic constants already represent a second-order quantity with respect to the total energy, Table II illustrates the importance of aiming for the highest possible numerical precision when conducting calculations of elastic constants. When it comes to reliability and precision, however, a recent meta-study [92] confirms that all-electron codes like WIEN2K represent the past as well as current state-of-the-art.

As a further caveat, we note that unfortunately the procedure implemented to calculate elastic constants in the Charpin package is not based on the use of the Lagrangian strain tensor required in the proper definition of elastic constants [36], but only on the linearized strain tensor. While this subtle difference is irrelevant at zero pressure, at nonzero external pressure such an approach actually yields the so-called Voigt elastic constants $V_{ijkl}[\boldsymbol{X}_P]$ which differ from the sought-after elastic constants $C_{ijkl}[\boldsymbol{X}_P]$ by [93]

$$C_{ijkl}[\boldsymbol{X}_P] = V_{ijkl}[\boldsymbol{X}_P] + \frac{P}{2}(\delta_{ik}\delta_{jl} + \delta_{il}\delta_{jk}). \qquad \text{(B1)}$$

Without this important correction (i.e. accidently identifying the tensors $C_{ijkl}[\boldsymbol{X}_P]$ and $V_{ijkl}[\boldsymbol{X}_P]$), the "elastic constants" obtained differ from the correct values by systematic errors of order no less than P. We have found this to be a pitfall to which even some prominent DFT-based codes seem to be vulnerable. Whenever in doubt, a calculated set of elastic constants can be numerically checked for consistency with an underlying EOS by (i) computing the corresponding set of Birch coefficients $B_{\mu\nu}[\boldsymbol{X}_P]$ from Eqs. (C5) and (C6), (ii) inverting the resulting tensor to obtain the compliances $S_{\mu\nu}[\boldsymbol{X}_P]$, and (iii) making use of the general relation $K(P) = 1/\sum_{\mu,\nu=1}^{3} S_{\mu\nu}[\boldsymbol{X}_P]$ to obtain the bulk modulus $K(P)$, which can be compared to the corresponding value directly obtained from the EOS [94].

Having determined the set of Birch coefficients $B_{\mu\nu}[\boldsymbol{X}_P]$, it is also straightforward to determine the pressure-dependent Poisson ratio $\sigma(P)$ as described in Appendix C. For PTO, using the PBEsol functional, we find that the ambient-pressure value of $\sigma \approx 0.28$ (cf. inset of Fig. 9) is only slightly in excess of the GIBBS2 default value $\sigma = 1/4$ corresponding to a Cauchy solid [53]. Within the calculated pressure range $0 \leqslant P \leqslant 20$ GPa we also note a weak, roughly linear rise of σ to $\sigma \approx 0.31$ at $P = 20$ GPa. The observed overall dependence of the DA on σ is, however, observed to be quite weak. Therefore we settled for a value of $\sigma = 0.28$, which was used subsequently in the DA.

TABLE II. Comparison of $T = 0$ *ab initio* results for ambient-pressure elastic constants of cubic PTO (NCPP=norm-conserving pseudopotential, USPP = ultrasoft pseudopotential, LCAO = linear combination of atomic orbitals, HF = Hartree-Fock, included here for comparison).

Ref.	Method	XC functional	Remarks	a_0 (Å)	C^0_{11} (GPa)	C^0_{12} (GPa)	C^0_{44} (GPa)	K_0 (GPa)
[79]	HF		LCAO (CRYSTAL)	3.94	398.3	169.0	172.0	245.4
[42]	DFT	LDA	USPP	3.889	341.4	148.8	102.7	208.9
[46]	DFT	LDA	NCPP (CASTEP 2.1)	3.883	320.2	141.2	187.4	203.0
[79]	DFT	LDA	LCAO (CRYSTAL)	3.93	450.3	261.4	112.8	324.3
[80]	DFT	LDA	NCPP (ABINIT)	4.090	321.7	113.3	83.9	179.7
this work	DFT	LDA	APW+lo (WIEN2K)	3.888	352.8	133.7	104.4	206.7
[79]	DFT	PBE	LCAO (CRYSTAL)	3.96	342.3	155.2	109.6	217.5
this work	DFT	PBE	APW+lo (WIEN2K)	3.970	282.0	117.3	97.1	172.2
this work	DFT	PBEsol	APW+lo (WIEN2K)	3.923	321.1	125.5	100.9	190.7

APPENDIX C: NOTES ON OUR USE OF THE DEBYE APPROXIMATION

Recall [61,95] that the DA replaces the original system by an effective isotropic model containing only acoustic phonons. From their longitudinal and transverse sound velocities v_P, v_S, respectively, one defines a directionally averaged sound velocity $\bar{v}$ with

$$\frac{3}{\bar{v}^3} = \frac{1}{v_P^3} + \frac{2}{v_S^3}. \tag{C1}$$

Given the mass density ρ, the bulk modulus K, and the Poisson ratio [96] σ, Slater [97] has shown that

$$\bar{v} = f(\sigma)\sqrt{K/\rho}, \tag{C2}$$

where

$$f(\sigma) \equiv \sqrt[3]{3}\left[\left(\frac{1+\sigma}{3(1-\sigma)}\right)^{\frac{3}{2}} + 2\left(\frac{2(1+\sigma)}{3(1-2\sigma)}\right)^{\frac{3}{2}}\right]^{-\frac{1}{3}}; \tag{C3}$$

ρ and K may be directly extracted from a given EOS while σ usually [53] takes values around 0.25 and exhibits only a very weak volume dependence.

Bearing in mind that the Debye approximation rests on approximating the underlying system as isotropic, it may not be obvious which value to plug into (C2) for the Poisson ratio σ, since in a crystal this represents, of course, a direction-dependent combination of elastic constants. Indeed it has been shown [98] that the Debye temperature may be calculated with excellent accuracy using the Voigt-Reuss-Hill (VRH) averaging scheme [99] of elastic constants which had been primarily invented to assess the elastic properties of granular material consisting of randomly oriented microcrystallites. In detail, given a crystal with elastic constants $C_{\mu\nu}$ and corresponding compliances $S_{\mu\nu}$, one defines Voigt (V), Reuss (R), and VRH averages of the bulk modulus K, the shear modulus G, and Poisson's ratio σ. Our present purposes only require the cubic formulas, for which the Voigt and Reuss averages both agree with the unaveraged result $K_V = K_R = K$, whereas one obtains $5G_V = (C_{11} - C_{12}) + 3C_{44}$ and $5/G_R = 4(S_{11} - S_{12}) + 3S_{44}$. From their arithmetic average $G_{VRH} = (G_V + G_R)/2$ one finally obtains a VRH-averaged Poisson ratio

$$\sigma \equiv \sigma_{VRH} = \frac{1}{2}\left(1 - \frac{3G_{VRH}}{3K + G_{VRH}}\right) \tag{C4}$$

in accordance with the formulas of standard elasticity theory (cf. Ref. [100]). In our present context, the elastic constants $C_{\mu\nu}$ entering the Voigt-Reuss-Hill formulas should, however, be replaced by the corresponding Birch coefficients $B_{\mu\nu}[\boldsymbol{X}_P]$. This follows from the observation that at nonzero pressure the B_{ij} are the tensor components that actually enter into the Christoffel equations determining the acoustic sound velocities (see Ref. [36]). In passing we note that for hydrostatic pressure $\sigma_{ij} = -P\delta_{ij}$ (and only then) the Birch coefficients (24) can indeed be written in Voigt notation as [36]

$$B_{\alpha\beta}[\boldsymbol{X}_P] = C_{\alpha\beta}[\boldsymbol{X}_P] + \Delta_{\alpha\beta}(P), \tag{C5}$$

TABLE III. Comparison of various results for cubic bulk modulus of PTO at $T = T_c$.

Ref.	Method	K_0 (GPa)
[65]	synchrotron x-ray diffraction	237(4)
[106]	synchrotron x-ray diffraction	195(3)
[33]	synchrotron x-ray diffraction	141(5)
[107]	Brillouin scattering	143.6
this work	DFT PBEsol+DA, $\sigma = 0.28$	161.3

where

$$\Delta(P) = \begin{pmatrix} -P & P & P & & & & \\ P & -P & P & & & & \\ P & P & -P & & & & \\ & & & -P & & & \\ & & & & -P & & \\ & & & & & -P & \end{pmatrix}. \tag{C6}$$

A complication worth mentioning is that the assumption that σ is completely independent of volume should, as already noted by Slater [97], result in an improper QHA. Attempts to fix this yield the class of so-called Debye-Grueneisen approximations [52,53], notably the Dugdale-McDonald [101], Vaschenko-Zubarev [102], and mean-free-volume [103,104] approximations (see Ref. [105] for details). All of these have been implemented in the computer code GIBBS2 [52,53], which—depending on the details of the available phonon information—also supports various other levels of the QHA as well as high-quality fitting routines for a large number of popular types of EOSs. As mentioned in Sec. V, the combination of PBEsol with a simple DA based on a Poisson ratio of $\sigma = 0.28$ yields the overall best agreement to the available volume data. For comparison, Table III also lists some experimental results on the bulk modulus of the cubic phase.

Even after having successfully promoted the EOS of the background system $\boldsymbol{X}_P$ from zero to finite temperature, we are still left with determining the much more difficult problem of also determining the T dependence of the corresponding background elastic constants $C_{ijkl}[\boldsymbol{X}_P] = C_{ijkl}[\boldsymbol{X}_P(T)]$. Our strategy to overcome this final obstacle is reminiscent of the one put together in Ref. [38] for the purpose of parametrizing an unknown P dependence of elastic constants. We start by observing that since the T dependence of the bulk modulus $K(P,T)$ is fully determined from the EOS based on our choice PBEsol+DA, the identity $1/K[\boldsymbol{X}_P](T) = \sum_{\mu,\nu=1}^{3} S_{\mu\nu}[\boldsymbol{X}_P](T)$ can be regarded as a constraint for any possible T variations of the elastic constants $C_{\mu\nu}[\boldsymbol{X}_P]$ for $\mu,\nu = 1,2,3$. Given a set of compliances $S_{ij}[\boldsymbol{X}_P](T=0)$ calculated from DFT, the compliances from the left upper quadrant $\mu,\nu \leqslant 3$ satisfy

$$S_{\mu\nu}[\boldsymbol{X}_P](T) = \frac{K[\boldsymbol{X}_P](0)}{K[\boldsymbol{X}_P](T)} S_{\mu\nu}[\boldsymbol{X}_P](T) + \cdots. \tag{C7}$$

Of course, the T dependence of transverse elastic constants like $C_{\mu\mu}$, $\mu = 4,5,6$ cannot be expected to be assessed in the

above way. Fortunately, in the transition under investigation shear strains play no role, so this is of no concern for our present problem.

Taking the example of a cubic system, this leaves a single function $\delta S(P,T)$ that accounts for any possible remaining trade-off between the compliance tensor components $S_{11}[\boldsymbol{X}_P](T)$ and $S_{12}[\boldsymbol{X}_P](T)$ not covered by the overall factor $K[\boldsymbol{X}_P](0)/K[\boldsymbol{X}_P](T)$. Since this function must vanish for $T = 0$, it follows that it might be possible to expand $\delta S(P,T)$ into a power series in T with P-dependent coefficients. However, for our present purposes we refrain from introducing such further complications and content ourselves with the lowest order approximation as indicated in Eq. (C7). Results are included in Table III.

Owing to the fact that the cubic phase is only thermodynamically stable above T_c, published experimental data on the cubic elastic constants of PTO are rather scarce. In the DFT-related literature (cf., e.g., Refs. [79,108,109]), Brillouin scattering results $C_{11} \approx 229$ GPa, $C_{12} \approx 101$ GPa, and $C_{44} \approx 100$ GPa for the cubic phase are frequently attributed to Ref. [107]. Actually, however, the value of C_{12} reported in Ref. [107] refers only to the room-temperature tetragonal phase, while we are unable to spot any explicit value for the cubic elastic constant C_{12} in Ref. [107]. We therefore suspect that the above frequently cited value for C_{12} represents only a conjecture vaguely related to the observation that the value of the tetragonal elastic constant $C_{13} \approx 98.8$ GPa reported in Ref. [107] almost agrees with said value of C_{12}. Adopting this hypothesis for the moment, one would derive a cubic bulk modulus of $K_0 \approx 143.6$ GPa. On the other hand, using the simple strategy outlined in Eq. (C7) to extrapolate our DFT results to T_c, we obtain the numbers $C_{11}^0 \approx 271$ GPa and $C_{12}^0 \approx 106$ GPa yielding a bulk modulus $K_0 \approx 161.3$ GPa in reasonable agreement with and certainly in the same ballpark as the experimental results gathered in Table III.

It is interesting to compare these results to the compliance values $S_{11}^0 = 8.0 \times 10^{-12}\,\mathrm{m^2/N}$ and $S_{12}^0 = -2.5 \times 10^{-12}\,\mathrm{m^2/N}$ listed in the very influential paper Ref. [26] and reproduced in a number of subsequent publication by other authors (see, e.g., Refs. [13,27]). Inverting the compliance tensor, we obtain values $C_{11}^0 = 174.6$ GPa, $C_{12}^0 = 79.3$ GPa, and $K = 111.11$ GPa that are much lower than those listed above. Puzzled by this discrepancy, we traced the origin of these values, which the authors of Ref. [26] had themselves taken from other sources, back to Ref. [28], which also lists the same value for S_{12}^0 as Ref. [26] but for S_{11}^0 gives a value of $S_{11}^0 = 6.785 \times 10^{-12}\,\mathrm{m^2/N}$ instead. This set of compliances now results in $C_{11}^0 = 258.5$ GPa and $C_{12}^0 = 150.8$ GPa with an accompanying bulk modulus of $K = 186.7$ GPa, in much better agreement with the values listed before. Some readers may find this discussion lengthy. However, while we are only speculating about the actual source of the detected discrepancy; in any case such sizable errors in the values of elastic constants may have the potential to seriously affect the results of, e.g., calculations dealing with uniaxial stresses appearing in epitaxial layers of PTO on substrates. For the Landau theory of the ferroelectric transition at ambient pressure, these problems are fortunately of no concern, since for $P = 0$ the values of the elastic constants drop out of the corresponding calculations. In summary, there is clear evidence that not only the values of the couplings q_μ but also the compliances S_{11}, S_{12}, and S_{44} need to be revised in the published tables of Landau parameters for PTO.

APPENDIX D: REDEFINING THE ELASTIC BASELINE

Any time a LT contains secondary order parameters, a definition of their spontaneous equilibrium values should always require defining a corresponding baseline in advance. A correct definition of the spontaneous strain components from a given set of P-dependent unit cell parameters thus relies on the determination of a meaningful elastic reference system $\boldsymbol{X}_P(T)$ together with a compatible set of elastic constants $C_{\mu\nu}[\boldsymbol{X}_P(T)]$, and Appendix C summarizes our corresponding efforts. In principle, only then fits of (4) to the resulting spontaneous strain data allow us to obtain the strain-OP coupling coefficients $\widehat{q}_\mu$. This raises the question of how Haun *et al.* had overcome this difficulty in the first place without having to go through all the arguments we have given above. A careful reading of their paper reveals that the answer to this question is disarmingly simple. In fact, their baseline has been defined *a posteriori* based on the convenient requirement that the proportionality factors between the squared OP and the spontaneous strain components, which are just the Landau coefficients $\widehat{q}_\mu$ according to Eq. (11), should be constants independent of T. Our present baseline preserves this proportionality, albeit with a new set of coupling coefficients $\widehat{q}_\mu = \widehat{q}_\mu(T)$ that are now inevitably T-dependent. For a DA with $\sigma = 0.28$, a rough polynomial fit up to second order produces (Fig. 4)

$$\widehat{q}_{11}(T) \approx +0.098\,16 - 9.764 \times 10^{-6}\,T + 6.11 \times 10^{-9}\,T^2,$$
$$\widehat{q}_{12}(T) \approx -0.020\,55 + 1.486 \times 10^{-5}\,T - 2.561 \times 10^{-8}\,T^2. \tag{D1}$$

[1] M. Murakami, K. Hirose, K. Kawamura, N. Sata, and Y. Ohishi, Science **304**, 855 (2004).

[2] A. Jaffe, Y. Lin, C. M. Beavers, J. Voss, W. L. Mao, and H. I. Karunadasa, ACS Central Science **2**, 201 (2016).

[3] H. J. Zhao, X. Q. Liu, X. M. Chen, and L. Bellaiche, Phys. Rev. B **90**, 195147 (2014).

[4] H. Sharma, J. Kreisel, and P. Ghosez, Phys. Rev. B **90**, 214102 (2014).

[5] E. Gilioli and L. Ehm, IUCrJ **1**, 590 (2014).

[6] J. Tolédano and P. Tolédano, *The Landau Theory of Phase Transitions* (World Scientific, Singapore, 1987).

[7] L. Landau, E. Lifshitz, and L. Pitaevskii, *Statistical Physics*, Part I (Butterworth and Heinemann, Oxford, 2001).

[8] M. Lines and A. Glass, *Principles and Applications of Ferroelectrics and Related Materials* (Clarendon Press, Oxford, 1977).

[9] T. Duffy, Nature (London) **506**, 427 (2014).
[10] A. Tröster, W. Schranz, F. Karsai, and P. Blaha, Phys. Rev. X **4**, 031010 (2014).
[11] B. Karki, L. Stixrude, and R. Wentzcovitch, Rev. Geophys. **39**, 507 (2001).
[12] A. Togo, F. Oba, and I. Tanaka, Phys. Rev. B **78**, 134106 (2008).
[13] *Physics of Ferroelectrics*, Vol. 105 of Topics in Applied Physics, edited by K. Rabe, C. Ahn, and J.-M. Triscone (Springer, Berlin, 2007).
[14] B. Noheda, Curr. Opin. Solid State Mater. Sci. **6**, 27 (2002).
[15] Z. Kutnjak, J. Petzelt, and R. Blinc, Nature (London) **441**, 956 (2006).
[16] G. Shirane, S. Hoshino, and K. Suzuki, Phys. Rev. **80**, 1105 (1950).
[17] G. Shirane and S. Hoshino, J. Phys. Soc. Jpn. **6**, 265 (1951).
[18] G. Shirane, J. D. Axe, J. Harada, and J. P. Remeika, Phys. Rev. B **2**, 155 (1970).
[19] G. Burns and B. A. Scott, Phys. Rev. Lett. **25**, 167 (1970).
[20] G. Burns and B. A. Scott, Phys. Rev. B **7**, 3088 (1973).
[21] J. Remeika and A. Glass, Mater. Res. Bull. **5**, 37 (1970).
[22] A. Amin, M. J. Haun, B. Badger, H. McKinstry, and L. E. Cross, Ferroelectrics **65**, 107 (1985).
[23] M. J. Haun, E. Furman, S. J. Jang, H. A. McKinstry, and L. E. Cross, J. Appl. Phys. **62**, 3331 (1987).
[24] A. F. Devonshire, The London, Edinburgh, and Dublin Philosophical Magazine and Journal of Science **40**, 1040 (1949).
[25] D. Vanderbilt and M. H. Cohen, Phys. Rev. B **63**, 094108 (2001).
[26] N. A. Pertsev, A. G. Zembilgotov, and A. K. Tagantsev, Phys. Rev. Lett. **80**, 1988 (1998).
[27] J. Gao, F. Li, Z. Xu, C. Zhang, Y. Liu, G. Liu, T. Zhang, and H. He, J. Phys. D **46**, 215304 (2013).
[28] G. A. Rossett, K. R. Udayakumar, M. J. Haun, and L. E. Cross, J. Am. Ceram. Soc. **73**, 3334 (1990).
[29] J. A. Sanjurjo, E. López-Cruz, and G. Burns, Phys. Rev. B **28**, 7260 (1983).
[30] P.-E. Janolin, P. Bouvier, J. Kreisel, P. A. Thomas, I. A. Kornev, L. Bellaiche, W. Crichton, M. Hanfland, and B. Dkhil, Phys. Rev. Lett. **101**, 237601 (2008).
[31] R. J. Nelmes and A. Katrusiak, J. Phys. C **19**, L725 (1986).
[32] P. Pruzan, D. Gourdain, and J. C. Chervin, Phase Transitions **80**, 1103 (2007).
[33] J. Zhu, H. Xu, J. Zhang, C. Jin, L. Wang, and Y. Zhao, J. Appl. Phys. **110**, 084103 (2011).
[34] M. Ahart, M. Somayazulu, R. E. Cohen, P. Ganesh, P. Dera, H.-k. Mao, R. J. Hemley, Y. Ren, P. Liermann, and Z. Wu, Nature (London) **451**, 545 (2008).
[35] P. Ganesh and R. E. Cohen, J. Phys.: Condens. Matter **21**, 064225 (2009).
[36] D. Wallace, *Thermodynamics of Crystals* (Dover, New York, 1998).
[37] J. W. Morris and C. R. Krenn, Philos. Mag. A **80**, 2827 (2000).
[38] A. Tröster, W. Schranz, and R. Miletich, Phys. Rev. Lett. **88**, 055503 (2002).
[39] Z. Wu and R. E. Cohen, Phys. Rev. Lett. **95**, 037601 (2005).
[40] I. A. Kornev, L. Bellaiche, P. Bouvier, P.-E. Janolin, B. Dkhil, and J. Kreisel, Phys. Rev. Lett. **95**, 196804 (2005).
[41] I. A. Kornev and L. Bellaiche, Phase Transitions **80**, 385 (2007).
[42] R. D. King-Smith and D. Vanderbilt, Phys. Rev. B **49**, 5828 (1994).
[43] K. M. Rabe and J. D. Joannopoulos, Phys. Rev. Lett. **59**, 570 (1987).
[44] W. Zhong, D. Vanderbilt, and K. M. Rabe, Phys. Rev. Lett. **73**, 1861 (1994).
[45] W. Zhong, D. Vanderbilt, and K. M. Rabe, Phys. Rev. B **52**, 6301 (1995).
[46] U. V. Waghmare and K. M. Rabe, Phys. Rev. B **55**, 6161 (1997).
[47] A. Kumar, K. M. Rabe, and U. V. Waghmare, Phys. Rev. B **87**, 024107 (2013).
[48] H. Krakauer, R. Yu, C.-Z. Wang, K. M. Rabe, and U. V. Waghmare, J. Phys.: Condens. Matter **11**, 3779 (1999).
[49] S. Tinte, J. Íñiguez, K. M. Rabe, and D. Vanderbilt, Phys. Rev. B **67**, 064106 (2003).
[50] A. D. Bruce and R. A. Cowley, *Structural Phase Transitions* (Taylor and Francis Ltd., London, 1981).
[51] O. Anderson, *Equations of State of Solids for Geophysics and Ceramic Science* (Oxford University Press, Oxford, 1995).
[52] A. Otero-de-la-Roza and V. Luaña, Comput. Phys. Commun. **182**, 1708 (2011).
[53] A. Otero-de-la-Roza, D. Abbasi-Pérez, and V. Luaña, Comput. Phys. Commun. **182**, 2232 (2011).
[54] M. Dove, *Introduction to Lattice Dynamics* (Cambridge University Press, Cambridge, 2004).
[55] B. Fultz, *Phase Transitions in Materials* (Cambridge University Press, Cambridge, 2014).
[56] O. Hellman, I. A. Abrikosov, and S. I. Simak, Phys. Rev. B **84**, 180301 (2011).
[57] P. Souvatzis, S. Arapan, O. Eriksson, and M. I. Katsnelson, Europhys. Lett. **96**, 66006 (2011).
[58] S. W. Kieffer, Rev. Geophys. **17**, 1 (1979); **17**, 20 (1979); **17**, 35 (1979); **18**, 862 (1980); **20**, 827 (1982).
[59] A. Oganov, in *Treatise on Geophysics*, edited by G. Schubert (Elsevier, Amsterdam, 2007), pp. 121–152.
[60] L. Stixrude and R. Jeanloz, in *Treatise on Geophysics*, edited by G. Schubert (Elsevier, Amsterdam, 2007), pp. 775–803.
[61] *An Introduction to High-Pressure Science and Technology*, edited by J. M. Recio, J. M. Menendez, and A. Otero-de-la-Roza (CRC Press, Boca Raton, FL, 2016).
[62] A. Tröster, Phys. Rev. Lett. **100**, 140602 (2008).
[63] E. Salje, *Phase Transitions in Ferroelastic and Coelastic Crystals* (Cambridge University Press, Cambridge, 1990).
[64] R. Ramirez, M. F. Lapena, and J. A. Gonzalo, Phys. Rev. B **42**, 2604 (1990).
[65] A. Sani, M. Hanfland, and D. Levy, J. Solid State Chem. **167**, 446 (2002).
[66] S. G. Jabarov, D. P. Kozlenko, S. E. Kichanov, A. I. Mamedov, R. Z. Mehdieva, E. V. Lukin, B. N. Savenko, and C. Lathe, Surface Engineering and Applied Electrochemistry **48**, 69 (2012).
[67] G. A. Samara, Ferroelectrics **2**, 277 (1971).
[68] A. Tröster, C. Dellago, and W. Schranz, Phys. Rev. B **72**, 094103 (2005).
[69] A. Tröster and C. Dellago, Ferroelectrics **354**, 225 (2007).
[70] P. Souvatzis, O. Eriksson, M. I. Katsnelson, and S. P. Rudin, Phys. Rev. Lett. **100**, 095901 (2008).
[71] J. C. Thomas and A. Van der Ven, Phys. Rev. B **88**, 214111 (2013).

[72] V. I. Levitas, D. L. Preston, and D.-W. Lee, Phys. Rev. B **68**, 134201 (2003).
[73] V. I. Levitas, Int. J. Plast. **49**, 85 (2013).
[74] V. A. Levin, V. I. Levitas, K. M. Zingerman, and E. I. Freiman, Int. J. Solids Struct. **50**, 2914 (2013).
[75] V. I. Levitas, J. Mech. Phys. Solids **70**, 154 (2014).
[76] A. Vattré and C. Denoual, J. Mech. Phys. Solids **92**, 1 (2016).
[77] C. Denoual and A. Vattré, J. Mech. Phys. Solids **90**, 91 (2016).
[78] P. Toledano and V. Dmitriev, *Reconstructive Phase Transitions in Crystals and Quasicrystals* (World Scientific, Singapore, 1996).
[79] S. Piskunov, E. Heifets, R. Eglitis, and G. Borstel, Comput. Mater. Sci. **29**, 165 (2004).
[80] W. Huang, H. Yang, G. Lu, and Y. Gao, Physica B **411**, 56 (2013).
[81] P. Blaha, K. Schwarz, G. K. H. Madsen, D. Kvasnicka, and J. Luitz, *WIEN2k: An Augmented Plane Wave and Local Orbitals Program for Calculating Crystal Properties* (Vienna University of Technology, Austria, 2001).
[82] D. Singh and L. Nordström, *Planewaves, Pseudopotentials and the LAPW Method*, 2nd ed. (Springer, New York, 2006).
[83] Z. Wu, R. E. Cohen, and D. J. Singh, Phys. Rev. B **70**, 104112 (2004).
[84] Z. Wu and R. E. Cohen, Phys. Rev. B **73**, 235116 (2006).
[85] J. P. Perdew, A. Ruzsinszky, G. I. Csonka, O. A. Vydrov, G. E. Scuseria, L. A. Constantin, X. Zhou, and K. Burke, Phys. Rev. Lett. **100**, 136406 (2008).
[86] F. Tran, R. Laskowski, P. Blaha, and K. Schwarz, Phys. Rev. B **75**, 115131 (2007).
[87] J. P. Perdew, K. Burke, and M. Ernzerhof, Phys. Rev. Lett. **77**, 3865 (1996).
[88] J. P. Perdew, K. Burke, and M. Ernzerhof, Phys. Rev. Lett. **78**, 1396 (1997).
[89] R. Wahl, D. Vogtenhuber, and G. Kresse, Phys. Rev. B **78**, 104116 (2008).
[90] F. Birch, Phys. Rev. **71**, 809 (1947).
[91] A. van de Walle and G. Ceder, Phys. Rev. B **59**, 14992 (1999).
[92] K. Lejaeghere *et al.*, Science **351**, aad3000 (2016).
[93] D. C. Wallace, Phys. Rev. **162**, 776 (1967).
[94] J. Koppensteiner, A. Tröster, and W. Schranz, Phys. Rev. B **74**, 014111 (2006).
[95] J.-P. Poirier, *Introduction to the Physics of the Earth's Interior*, 2nd ed. (Cambridge University Press, Cambridge, 2000).
[96] G. N. Greaves, A. L. Greer, R. S. Lakes, and T. Rouxel, Nat. Mater. **10**, 823 (2011).
[97] J. Slater, *Introduction to Chemical Physics* (McGraw-Hill, New York, 1939).
[98] O. L. Anderson, J. Phys. Chem. Solids **24**, 909 (1963).
[99] R. Hill, Proc. Phys. Soc., London, Sect. A **65**, 349 (1952).
[100] G. Grimvall, *Thermophysical Properties of Materials* (Elsevier, Amsterdam, 1999).
[101] J. S. Dugdale and D. K. C. MacDonald, Phys. Rev. **89**, 832 (1953).
[102] V. Vashenko and V. Zubarev, Sov. Phys. Solid State **5**, 653 (1963).
[103] M. A. Barton and F. D. Stacey, Phys. Earth Planet. Inter. **39**, 167 (1985).
[104] F. D. Stacey, Phys. Earth Planet. Inter. **89**, 219 (1995).
[105] L. Vočadlo, J. Poirier, and G. Price, Am. Mineral. **85**, 390 (1985).
[106] A. Sani, M. Hanfland, and D. Levy, J. Phys.: Condens. Matter **14**, 10601 (2002).
[107] Z. Li, M. Grimsditch, C. Foster, and S.-K. Chan, J. Phys. Chem. Solids **57**, 1433 (1996).
[108] J. Long, L. Yang, and X. Wei, J. Alloys Compd. **549**, 336 (2013).
[109] Y. Liu, G. Xu, C. Song, Z. Ren, G. Han, and Y. Zheng, Mater. Sci. Eng., A **472**, 269 (2008).